AD-765 350

ATMOSPHERIC PRESSURE GAS LASERS

Hermann A. Haus

Massachusetts Institute of Technology

Prepared for:

Advanced Research Projects Agency

26 January 1973

AD 765350

SEMIANNUAL TECHNICAL REPORT ON
ATMOSPHERIC PRESSURE GAS LASERS

covering the period

December 1, 1972 – May 31, 1973

submitted by

Hermann A. Haus
Professor of Electrical Engineering

Sponsored by

Advanced Research Projects Agency
ARPA Order No. 0675, Amend. No. 19

Contract Number: DAHC04-72-C-0044

Program Code No.:
62301E

Principal Investogator
Hermann A. Haus
617-253-2585

Contractor:

Massachusetts Institute of
Technology
Cambridge, Mass. 02139

Effective Date of Contract:

June 1, 1972

Expiration Date:

May 31, 1974

Amount of Contract:

$80,000

Short Title of Work:

Atmospheric-Pressure Gas Lasers

Date of Report:

January 26, 1973

The views and conclusions contained in this document are those of the authors, and should not be interpreted as necessarily representing the official policies, either expressed or implied, of the Advanced Research Projects Agency or the U.S. Government.

Approved for public release; distribution unlimited

Semiannual Technical Report on

Atmospheric Pressure Gas Lasers

covering the period

December 1, 1972 – May 31, 1973

SUMMARY

I. <u>Mode Locking and Pulse Selection</u>

In the previous semiannual report, work of Y. Manichaikul was
described in which he successfully switched out a single optical pulse
from a mode-locked CO_2 transversely excited atmospheric pressure (TEA)
laser. The peak pulse power was of the order of 10 kW.

A new system has been designed to produce short laser pulses in
order to improve the achievable peak powers and also to enable us to
obtain two optical pulses of roughly equal intensity separated by a time
of the order of 20 ns. Improvements in the peak powers were necessary
to enable saturation of a TEA amplifier with the pulse in order to study
nonlinear amplification in such a system; the selection of two (or more)
successive pulses was desirable, in order to ascertain the relaxation
times responsible for the recovery of the upper laser level through inter-
change of energy with other vibrational levels of the same vibrational
(asymmetric stretching) mode. The system has been operated success-
fully, giving pulses of less than 2 ns duration and 500 kW peak intensity.
The system is described in detail in Quarterly Progress Report No. 110,

Research Laboratory of Electronics, July 15, 1973; a revised version meantime appears as Appendix I of this report. We have now made extensive amplifier measurements which we are analyzing and will report subsequently.

In addition to forced mode locking by an acoustically driven crystal, mode locking by a saturable absorber (a hot CO_2 cell) promises to be a convenient means to produce short mode-locked pulses. Such work on conventional TEA lasers has been reported in the literature. The scheme is particularly attractive for the mode locking of lasers operating at 10 atm. Such a laser has recently been operated successfully in this research group by J. L. Miller. A gas cell has the obvious advantage over a crystal in that it is less susceptible to optical damage, which is a more critical requirement at the high intensities achieved with high-pressure lasers. The theory of mode locking by saturable absorbers, although widely discussed in the literature, is less well understood than the theory of forced mode locking. In an attempt to predict the operating requirements of the hot CO_2 cell, a theoretical analysis has been initiated of mode locking by saturable absorbers. Thus far, we have analyzed the case of a weakly saturated amplifying medium and a weakly saturated absorber, the latter with response times fast compared with mode-locked pulse time and amplifier response time. The theory is presented in Appendix II, a preprint from Quarterly Progress Report No. 110, Research Laboratory of Electronics, July 15, 1973.

2

II. Closed-Form Analysis of Electron Distribution and Pumping Rates

The analysis of the electron distribution in a discharge excited molecular laser mentioned in our previous semiannual report has been written up in a paper submitted to the Journal of Applied Physics; a copy of this paper constitutes Appendix III. Stated briefly, the objective of the work is to find simple analytic expressions for the electron distribution in the laser discharge, including the effect of lasing. Examples treated in the paper include, for an E-beam CO_2 laser, the evaluation of the V-I characteristic of the sustainer field, the gain, the efficiency and the pumping rates of the molecular levels with and without lasing.

3

GENERATION AND AMPLIFICATION OF HIGH-INTENSITY NANOSECOND TEA CO_2 LASER PULSES

Y. Manichaikul

We have reported previously on generation of short nanosecond pulses from a pin resistor TEA CO_2 laser by way of mode locking and cavity dumping.[1] Single pulses 4 ns wide (full width at half maximum, FWHM) with peak power ~10 kW were produced. Problems were encountered with the system and a new one was built. The problems, and the changes that have been made in the new system, are as follows.

(i) The peak power obtained from the previous system was too low for some experiments. For example, to saturate a TEA CO_2 laser amplifier requires a peak intensity greater than 100 kW/cm^2. In our new system we use a 3-electrode TEA CO_2 discharge tube which has a higher gain than the pin-resistor TEA CO_2 discharge tube.[2] With this improved system we have obtained mode-locked pulses of peak powers in excess of 500 kW.

(ii) A germanium acousto-optic modulator at Brewster angle is now being used. This eliminates the power-density limitation that

arose in the old system, which used an antireflection-coated germanium modulator.

(iii) An antireflection-coated GaAs crystal is now placed outside, rather than inside, the optical cavity, which makes alignment of the cavity less critical.

(iv) In the old system the high-voltage supply to the cavity-dumping GaAs crystal was falsely triggered by electrical noise generated by the laser discharge tube. In the new system a laser-induced spark gap[3] is used to eliminate this problem.

(v) Previously, continuous RF power was supplied to the germanium mode-locking crystal. This caused the germanium crystal to heat up, thereby changing its acoustic resonance frequencies. We are now using pulsed RF power to minimize this problem.

Experimental Arrangement

Figure 1 is a schematic diagram of the experimental arrangement. With a dc voltage of 5 kV across the GaAs electro-optic modulator a fraction of the energy from the beam can be switched out at the Brewster-angle germanium plate, Ge P. This fraction of the beam was guided by two flat mirrors to a gold-coated mirror with 2-m radius of curvature, which focuses the beam inside the 3-electrode laser amplifier. The tube is operated between 10 Torr and 400 Torr. A fraction of the beam, before going into the amplifier, is reflected out from a beam splitter and detected by a copper-doped liquid-helium-cooled detector with a rise time of <1 ns. The fraction of the beam that has

5

passed through the amplifier is detected by a gold-doped liquid-nitrogen-cooled detector with a rise time of ~1 ns.

Experiments

a. Generation of Nanosecond TEA CO_2 Laser Pulses

The laser cavity has an optical length of approximately 1.88 m. To achieve forced mode locking, RF driving power over time intervals of 2.5 ms duration with 4 W peak power was supplied to the germanium acousto-optic modulator. The 3-electrode discharge tube inside the cavity is set to trigger at 2 ms after the RF power is on. We have obtained mode-locked pulses < 2 ns wide (FWHM) with a peak power of ~500 kW.

The switching out of individual pulses is accomplished by using the laser-induced spark gap, which is normally filled with prepurified nitrogen at 100 psi. The coaxial cable was charged up to 15 kV. We can vary the temporal triggering of this gap by altering the nitrogen pressure, the distance between the two electrodes of the spark gap, or both. When the spark gap is triggered, a square voltage pulse of 7.5 kV, twice the length of cable, is produced. This pulse is supplied to the GaAs crystal, which rotates the polarization of the desired number of mode-locked pulses. These mode-locked pulses are then reflected out of the train at the Brewster-angle germanium plate.

b. Amplification of Nanosecond TEA CO_2 Laser Pulses

Three pulses from a train of mode-locked pulses were switched out and guided through an amplifier tube. These pulses were measured

6

before and after they propagated through the laser amplifier. Figure 2 shows input and output signals detected by copper-doped germanium detectors. The output signal was artificially delayed 100 ns by use of a coaxial delay line. By using the add-mode on a Tektronix 7904 oscilloscope, we were able to display both signals on a single trace.

In our preliminary studies we have found that the first pulse of our three laser pulses is of sufficient power density to saturate the laser amplifier. Further work on this aspect of the experiment will be described in a future report.

References

1. Semiannual Technical Report covering the period June 1, 1972 – November 30, 1972.

2. P. R. Pearson and H. M. Lamberton, "Atmospheric Pressure CO_2 Lasers Giving High Output Energy Per Unit Volume," IEEE J. Quant. Electronics, Vol. QE-8, No. 2, pp. 145-149, February 1972.

3. A. V. Nurmikko, IEEE J. Quant. Electronics, Vol. QE-7, No. 9, pp. 470-471, September 1971.

Fig. 1.   Diagram of experimental arrangement.
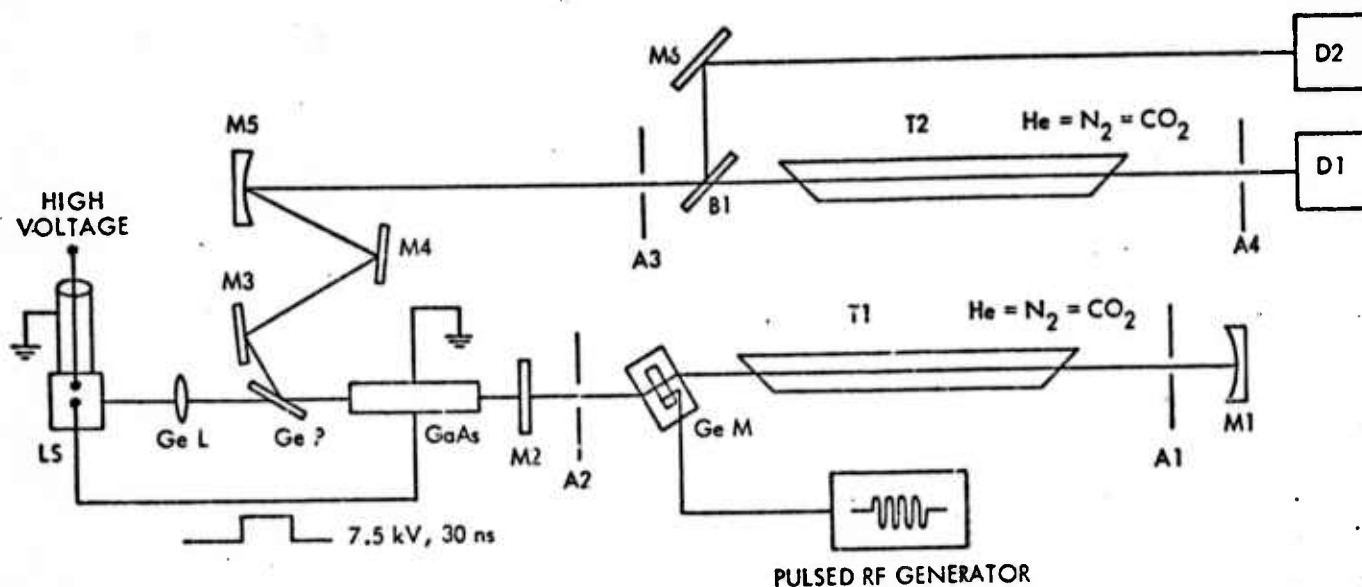
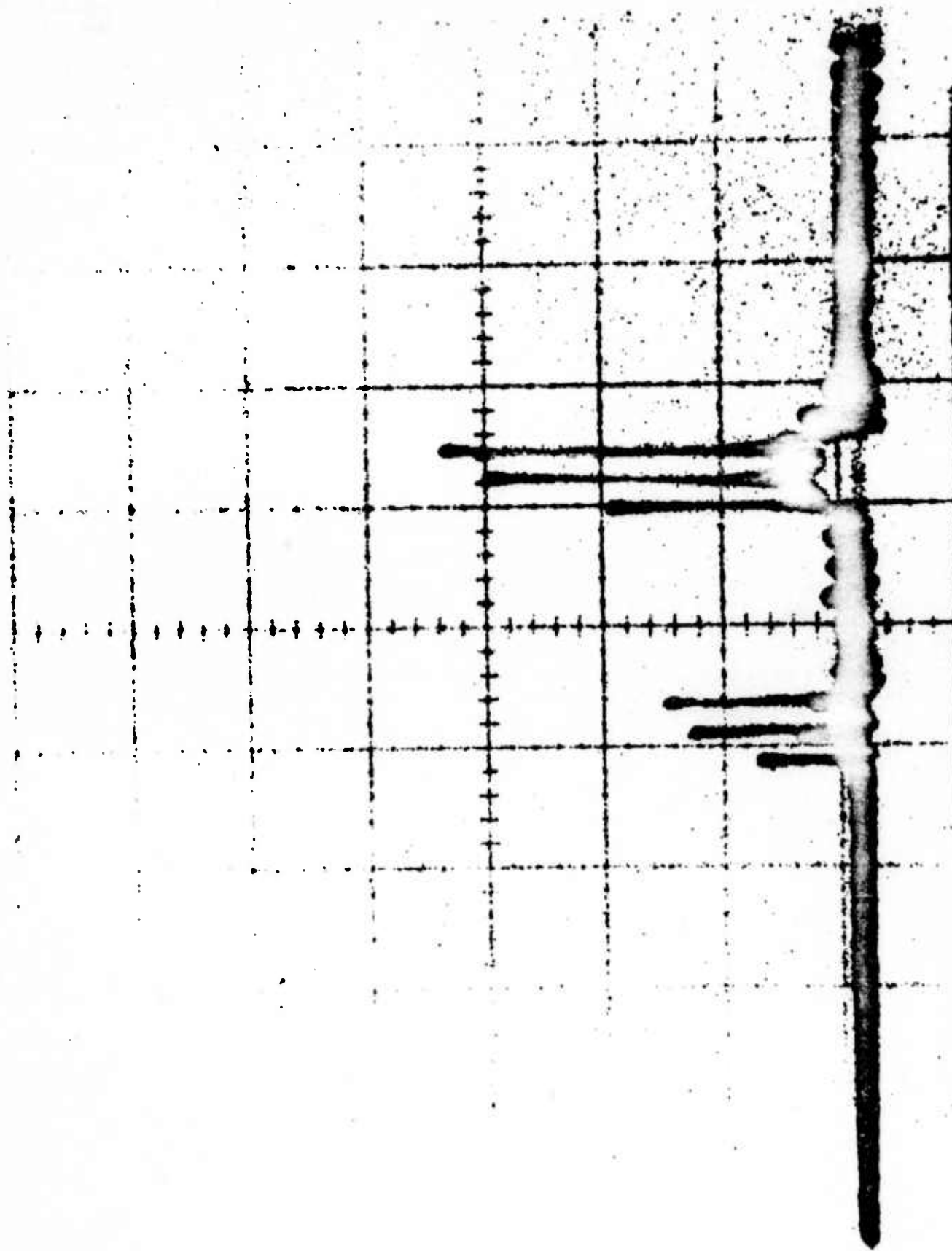| A1, A2, A3, A4	Apertures
B1	NaCl beam splitter
D1	Gold-doped detector
D2	Copper-doped detector
GaAs	Electro-optic modulator
Ge L	Germanium lens, 1.5" focal length
Ge M	Germanium acousto-optic modulator
Ge P	Germanium plate at Brewster angle
LS	Laser-induced spark gap
M1	Gold-coated mirror, 99.6 % reflecting, 4 m radius of curvature
M2	Germanium mirror, 20 % transmitting
M3, M4, M6	Gold-coated flat mirrors, totally reflecting
M5	Gold-coated mirror, 99.6 % reflecting, 2 m radius of curvature
T1, T2	3-electrode discharge tubes, 1 m long

Fig. 2. Input and output trains of the laser amplifier. An artificial 100 ns electrical delay facilitated the display (50 ns/div).

MODEL OF MODE LOCKING WITH SATURABLE ABSORBER

C. P. Ausschnitt, H. A. Haus

Of the many studies of mode locking using saturable absorbers, the
work of Kuizenga and Siegman[1] on forced mode locking has the greatest
analytic simplicity. In this report our objective is to obtain simple
expressions for the intensity and the pulse width of passively mode-locked
pulses and to choose a model simple enough to make closed-form analysis
possible. We assume, with Kuizenga and Siegman,[1] that the gain of the
laser medium changes negligibly through passage of a single pulse. We
further assume that the response time of the saturable absorber is fast
enough so that the population difference between the lower and upper levels
in the saturable absorber can follow the pulse envelope instantaneously.
Finally, we assume that the population perturbation in the saturable
absorber is small enough that its rate equation may be linearized.

Our analysis is analogous to Kuizenga and Siegman's and, in particu-
lar, we require that a Gaussian pulse reproduce in magnitude and width

after passage through the amplifier and the absorber and after reflection from the output mirror.

Adopting the notation of Kuizenga and Siegman and following their analysis of the passage of a Gaussian pulse through the amplifying medium, we obtain the electric field at the amplifier exit.

$$E = \frac{E_o G}{4\sqrt{\gamma A}} \exp\left[-(t-B)^2/4A\right].$$ (1)

When this pulse passes through the saturable absorber, it affects the population difference between the lower and upper levels of the absorber n according to the rate equation

$$\dot{n} + \frac{n - n^e}{T_1} = -\frac{T_2}{\hbar^2}|\mu|^2 n^e |E|^2.$$ (2)

All symbols in this equation refer to the parameters of the saturable absorber. Here n^e is the steady-state value of n.

Because the main pulse-shaping occurs near the maximum of an optical pulse, we expand the E-field of Eq. 1 around the instant at which E reaches a maximum and the absorption reaches a minimum. In this way, we obtain for the population difference in the absorber

$$n \approx n^e\left\{1 - \frac{|\mu|^2 T_1 T_2}{\hbar^2} \frac{E_o^2 G^2}{16\gamma A}\left[1 - 2(t-B)^2/4A\right]\right\}.$$ (3)

The signal passing through the absorber is multiplied by

$$\exp(-\alpha\ell) = \exp(-Sn),$$ (4)

11

where S is a parameter characteristic of the relaxation time and matrix elements of the absorber. At this point our analysis connects with the Kuizenga-Siegman analysis, since the modeling of the absorber makes it perform a function identical to the function performed by the modulator used in forced mode locking. The parameter $\delta_g \omega_m^2$ of Kuizenga and Siegman[1] is replaced by

$$\frac{I}{I_s} \frac{G^2}{16\gamma A^2} \frac{Sn^e}{4}, \tag{5}$$

where I_s is now the saturation intensity in the absorber. Using the results of Kuizenga and Siegman, from the self-consistency requirement on the pulse width we find

$$\gamma = \frac{1}{4A} + \frac{I}{I_s} \frac{G^2}{16\gamma A^2}. \tag{6}$$

The self-consistency requirement on the pulse amplitude gives

$$\frac{RG}{2\sqrt{\gamma A}} \exp(-Sn^e) = 1. \tag{7}$$

The parameter R is the reflectance of the output mirror. Solving these two equations for γ and the intensity I, and using $A = 1/(4\gamma) + 4g/\Delta\omega^2$, we obtain

$$\gamma \cong (L^2 G^2 - 1) \frac{\Delta\omega^2}{16g} \tag{8}$$

$$\frac{I}{I_s} = 4 \ln (R/L)(L^2 G^2 - 1)L^2, \tag{9}$$

12

where we have defined a loss parameter

$$L \equiv R \, \exp(-Sn^e).$$ (10)

The pulse-width parameter of Eq. 10 can be rewritten as a pulse duration time τ_p, which becomes

$$\tau_p = 8\sqrt{2 \ln 2} \, \sqrt{\frac{I_s}{I}} \, L \, \frac{\sqrt{g}}{\Delta \omega} \, \sqrt{\ln (R/L)}.$$ (11)

The parameters in Eq. 11 are identical to those used by Kuizenga and Siegman, with the exception of the loss parameter L, which now involves both the attenuation of the saturable absorber and the reflectance of the mirror, and I_s which is the saturation intensity of the absorber.

These results may be compared with published experiments on a TEA CO_2 laser that is mode-locked via a saturable absorber consisting of a heated CO_2 cell at a pressure higher than the amplifier pressure.[2] The assumptions here are generally consistent with these experimental conditions. The observed pulse length was 4 ns. If we introduce parameters that seem to match experimental results, we predict a pulse length ~1.5 ns. We believe that better agreement with experiment can be obtained if we generalize the analysis presented here to transient mode locking, by using an analysis analogous to Feldman's of transient forced mode locking.[3]

References

1. D. J. Kuizenga and A. E. Siegman, IEEE J. Quant. Electronics, Vol. QE-6, No. 11, pp. 694-708, November 1970.

2. A. F. Gibson, M. F. Kimmitt, and C. A. Rosito, Appl. Phys. Letters 18, 546-548 (1971).

3. S. J. Feldman, Private communication.

ELECTRON DISTRIBUTIONS IN GAS LASERS

W. P. Allis* and H. A. Haus**

Abstract

Simplified models of collision processes are introduced
which make possible closed form analyses of electron distri-
butions in molecular gases. In particular, models are con-
sidered that approximate the collision processes in a diatomic
gas and in a gas mixture resembling the $He:N_2:CO_2$ laser.
Expressions are obtained for the rates of excitation of the
vibrational modes which include the effect of superelastic
collisions. The results are illustrated by evaluating the
V-I characteristic and the efficiency of an E-beam CO_2 laser.

Introduction

In an effort to predict the gain and lasing efficiency
of CO and CO_2 lasers, computer studies have been carried out
to obtain the electron distribution and from it the pumping
rates in typical gas laser mixtures [1-5]. With such studies
it is possible to predict observed gains and efficiencies as

---

* Physics Department and Research Laboratory of Electronics,
M.I.T., Cambridge, Massachusetts 02139

** Electrical Engineering Department, and Research Laboratory
of Electronics, M.I.T., Cambridge, Massachusetts 02139

functions of excitation and gas mixtures.

Even though such computer studies are now available and numerical predictions can be made for any specific choice of parameters, it is still of interest to find models of gas lasers which permit closed form solutions and make possible easier identification of the influence of the various parameters. Here we present a model of interaction of electrons with diatomic and polyatomic molecules which permits closed form evaluation of the electron distribution. The population distributions of the molecules over their vibrational levels affect the electron distribution and vice versa. These effects are brought out clearly in the set of equations expressing the excitation rates in terms of electric field and the molecular population distribution. The results obtained for a diatomic laser are compared with computer results of Nighan [1] and we find reasonable agreement. A two-temperature model is developed for a mixture of CO_2 and nitrogen and is applied to obtain expressions for the V-I characteristic and efficiency for an E-beam CO_2 laser.

2. The Electron Gas

Electrons driven by a field E through a gas background tend to maintain a spherically symmetric velocity distribution as long as the electric field is not excessive. This is the

16

case for the values of E/N (where N is the number density of the gas) employed in gas laser discharges. We describe the electron distribution by the distribution function $f(\overline{v})$ where $\overline{v}$ is the vector velocity. In the usual analysis of $f(\overline{v})$, one separates $f(\overline{v})$ into a spherically symmetric part $f_0(\overline{v})$ (where v is the radial coordinate in velocity space, $v = |\overline{v}|$) and a part $f_1(\overline{E} \cdot \overline{v})$ which is the first higher order expansion term of $f(v)$ in a series of spherical harmonics. The steady state Boltzmann equation leads to two coupled first order differential equations in v for f_0 and f_1. Elimination of f_1 and disregard of the elastic collision losses leads to the following second order differential equation for $f_0(v)$ [1, 6]:

$$4\pi \frac{d}{dv} \left| \frac{v^2}{3} \frac{e}{m} \frac{E^2}{\nu_c} \frac{df_0}{dv} \right| = -4\pi v^2 \left(\frac{\partial f}{\partial t} \right)_{inel}$$

where ν_c is the frequency of momentum transfer collisions. The term on the left hand side represents the rate of entry of electrons into the velocity range v, v + dv produced by the driving electric field. The rate of entry of electrons is equal to the rate of exit caused by the inelastic collisions, the term on the right hand side of the equation. The distribution function $f_0(v)$ is normalized

$$\int 4\pi v^2 f_0(v) dv = 1 \qquad (2)$$

It is convenient to use as independent variable the energy in electron volts:

17

$$u = \frac{mv^2}{2e} \tag{3}$$

Further, it is convenient to renormalize $f_0(u)$ so that

$$\int f_0(v) \sqrt{u}\, du = 1 ,$$

a normalization which avoids factors of 2π and $2e/m$ in the equations. We shall henceforth omit the subscript 0. Note that

$$f(u) = 2\pi \left(\frac{2\dot{e}}{m}\right)^{3/2} f(v) .$$

We do not introduce a new symbol for $f(u)$, with the understanding that the variable used will identify which f is being employed. Renormalized, and with the change of variable, Eq. (1) becomes

$$\frac{d}{du} \left\{ \frac{2}{3} \frac{e}{m} \left(\frac{E}{\nu_c}\right)^2 \nu_c\, u^{3/2}\, \frac{df}{du} \right\} \tag{4}$$

$$= -\sqrt{u}\left(\frac{\partial f(u)}{\partial t}\right)_{inel} \qquad = - S_{inel} .$$

where the symbol S_{inel} is to imply a source of electrons per unit energy range as caused by inelastic collisions. The term in the wavy brackets is conveniently identified with a function $-G_E$

$$-G_E = \frac{2}{3} \frac{e}{m} \left(\frac{E}{\nu_c}\right)^2 \nu_c\, u^{3/2}\, \frac{df}{du} \tag{5}$$

This function has the interpretation of "current" in (one dimensional) energy space. Indeed, it obeys the one dimensional continuity equation:

$$\frac{dG_E}{du} = S_{inel} \tag{6}$$

where S_{inel} is a source rate per unit energy. The analogy with a "current" can be carried quite far. The divergence of a current density is equal to a source of particles. In the present case, the role of source is played by S_{inel} which represents the introduction of electrons per unit energy range via the inelastic collisions. This situation is illustrated schematically in Fig. 1. One may compare G_E to a conduction current density J driven by an electric field through a medium of conductivity σ. The "drive" in the present case is not E, but E^2. The quantity analogous to a conductivity is

$$-\frac{2}{3} \frac{e}{m} \frac{u^{3/2}}{\nu_c} \frac{df}{du}$$

This "conductivity" is, in general, positive. However, when $\frac{df}{du} > 0$, then instabilities may occur in energy space, very much like the instability in real space associated with a negative conductance.

Next consider inelastic collisions leading to electronic excitation. Suppose that electrons excite electronic levels of the atoms and/or molecules when they possess a sharply defined energy u_x. Electrons are being taken out of the energy range u_x, $u_x + du$ and we assume that they are returned with a

19

smaller energy at $u_x = u_x - V_x$; V_x is the energy of the excited transition. A source function may be defined for this process, S_x, which gives the rate of entry of electrons due to the electronic excitation process. If we further assume that all electronic excitations take place at u_x, this becomes a barrier beyond which electrons cannot go, and $f = 0$ for $u \geq u_x$.

$$S_x(u) = -[\nu_x \delta(u - u_x) - \nu_x \delta(u - u_x + V_x)] \quad (7)$$

Here, ν_x is the electronic excitation frequency and δ is the Dirac delta function.

In CO, the excitation of vibrational levels by the electrons occurs through the formation of a negative ion state. The excitation of the state requires 1.8 electron volts of energy. Upon excitation, the electrons lose an energy $\hbar\omega_a$ where $\hbar\omega_a$ is the vibrational energy interval, if the excitation carries the molecule from the 0 state to the 1 state. The energy loss is approximately $2\hbar\omega_a$ if the molecule is excited from the 0 to the 2 state, etc. We shall model the vibrational excitation process by assuming that all electrons lose an energy $V_a = \hbar\omega_a$ upon an exciting collision with a molecule, when they reach an energy $u_a + V_a$ (where $u_a = 1.8eV$ for CO); V_a will be assumed small enough when evaluating the differential equation for the distribution function, so that the source function S_a associated with molecular excitation,

20

$$S_a(u) = -[\nu_a \, \delta(u - u_a) - \nu_a \, \delta(u - u_a + V_a)]$$

$$(8)$$

may be approximated by a "doublet", a derivative of a delta function, $(\nu_a \to \infty, V_a \to 0)$. Note that ν_a represents the net vibrational "excitation" frequency due to both excitation and de-excitation. Now, returning to Eq. (4) we introduce explicitly the two source functions S_a and S_x.

$$\frac{dG_E}{du} = -\frac{d}{du} \left\{ \frac{2}{3} \frac{e}{m} \left(\frac{E}{\nu_c}\right)^2 \nu_c \, u^{3/2} \frac{df}{du} \right\} \qquad (9)$$

$$= S_x(u) + S_a(u)$$

A first integral of the equation gives

$$G_E = -\frac{2}{3} \frac{e}{m} \left(\frac{E}{\nu_c}\right) \nu_c \, u^{3/2} \frac{df}{du} = \int_0^u (S_x(u) + S_a(u)) du \qquad (10)$$

The integral of the source function is conveniently identified with a symbol of its own

$$\int_0^u S_x(u) \, du \equiv -G_x(u) \qquad (11)$$

$$\int_0^u S_a(u) \, du \equiv -G_a(u) \qquad (12)$$

These G functions themselves may be identified as currents in energy space whose divergence is responsible for the source of electrons. Indeed, the inelastic collisions also shuttle the electrons through energy space. A net arrival rate of electrons per unit energy is then caused by the negative divergence of the "currents" G_a and G_x which are produced by

21

the inelastic collisions. Indeed, Eqs. (11) and (12) may also be read as

$$\frac{dG_x}{du} = -S_x$$

$$\frac{dG_a}{du} = -S_a$$

One may now interpret Eq. (10) as requiring that, in the steady state, all currents in energy space must add up to zero.

$$G_E + G_a + G_x = 0 \tag{13}$$

This is shown schematically in Fig. 2. S_{inel} may be thought to be caused by $-\frac{d}{du} (G_a + G_x)$ which then in turn causes $+\frac{d}{du}G_E$.

It is convenient to think in terms of the functions G_a and G_x rather than in terms of S_a and S_x. The former are shown in Fig. 3. G_a is approximated by a unit impulse (delta) function whose area (content) may be obtained through simple physical reasoning. The energy supplied by the electrons through the collisions represented by S_a is

$$\int_o^u u\, S_a\, du = \int_o^u u\, \frac{dG_a}{du}\, du = u\, G_a \Big|_o^u - \int_o^u G_a\, du \tag{14}$$

22

$\int G_a du$ is the content of the delta function G_a.

From the above we may interpret

$$- \int_{0}^{u>u_a} G_a du \text{ as the energy } \nu_a V_a \text{ lost by the electrons}$$

Equation (13) may be rewritten as a differential equation for $f(u)$

$$-\frac{2}{3} \frac{e}{m} (\frac{E}{\nu_c})^2 \nu_c u^{3/2} \frac{df}{du} = -(G_x + G_a) \tag{15}$$

where $G_x + G_a$ is a known function consisting of the rectangle of height ν_x and the delta function of area $\nu_a V_a$ shown in Figure 3. In order to integrate it is necessary to know the collision frequency ν_c as a function of u. For simplicity we shall assume it to be constant and then the integral is easy and yields:

$$f(u) = \frac{\nu_x}{\nu_c} \frac{3}{2u_d} \{\frac{1}{\sqrt{u}} - \frac{1}{\sqrt{u_x}}\} \; ; \; u_a < u < u_x \tag{16}$$

$$= \frac{\nu_x}{\nu_c} \frac{3}{2u_d} \{\frac{1}{\sqrt{u}} - \frac{1}{\sqrt{u_x}} + \frac{\nu_a}{\nu_x} \frac{V_a}{2u_a^{3/2}}\}; u_x - V_x < u < u_a$$

where

$$u_d = \frac{1}{2} \frac{e}{m} (\frac{E}{\nu_c})^2 \tag{17}$$

is the drift velocity of the electrons expressed in electron volts. Note that u_d is proportional to the ratio $(E/N)^2$ The normalization condition (1) when utilized gives

$$\nu_x V_x + \nu_a V_a = \nu_c 2u_d \tag{18}$$

23

This is the law of energy conservation per particle. On the left hand side appears the rate of energy transfer to the electronic and vibrational excitations, on the right hand side is the power supplied by the electric field ($u_d \propto E^2$). One may combine (16) and (18) to eliminate v_a and obtain

$$f(u) = \left(\frac{V_x \nu_x}{2 u_d \nu_c}\right) \frac{3}{V_x} \left(\frac{1}{\sqrt{u}} - \frac{1}{\sqrt{u_x}}\right); \quad u_x > u > u_a$$

$$= \left(\frac{V_x \nu_x}{2 u_d \nu_c}\right) \frac{3}{V_x} \left(\frac{1}{\sqrt{u}} - \frac{1}{\sqrt{u_x}}\right)$$

$$+ \frac{3}{2 u_a^{3/2}} \left(1 - \frac{V_x \nu_x}{2 u_d \nu_c}\right); \quad v_a > u > u_x - V_x \quad (19)$$

Note that $V_x \nu_x / 2 u_d \nu_d$ is the fraction of the power absorbed which goes into electronic excitation and must be less than unity. The larger this parameter, the larger $f(u)$ in the range $u_a < u < u_x$. Figure 4 shows plots of $f(u)$ for different values of the excitation parameter $Exc \equiv \dfrac{V_x \nu_x}{2 u_d \nu_c}$. The following values have been chosen: $u_a = 2$ eV, $u_x = 10$ eV, $v_a = .2$ eV, $V_x = 10$. The entries E/N will be explained later.

One consequence of the simplifying assumptions is immediately evident. The electron distribution is pinned down at $u = u_x$ and is zero beyond. (If we had allowed for excitation levels above u_x, this would not have happened). Therefore our model is limited to F/N values for which most of the electrons have energies less than u_x and does not give information on electron densities at $u > u_x$. To obtain such information, for example, to compute ionization rates, one must do additional modeling as shown in section 9. Another interesting consequence of the model is that the electron energy parameter

as defined by Nighan

$$\bar{u}_r \equiv \frac{2}{3} \int u^{3/2} f(u) \, du$$

lies between the two extremes:

$$\lim_{E \to 0} \bar{u}_r = \frac{2}{5} u_a$$

$$\text{and } \lim_{E \to \infty} \bar{u}_r = \frac{u_x}{5}$$

In particular, in the limit of zero field the electrons still have a finite energy. This is a consequence of disregarding elastic losses. Hence our analysis is not applicable to very low fields either. Fortunately, in laser discharges the E/N values used are such that electron energies lie well between these two extremes and the approximations which led to these limits are acceptable.

Normalization provides one relation (18) between the unknown excitation rates ν_x and ν_a. The detailed molecular excitation processes considered in the next section will provide the second relation which is necessary to determine them.

3. Excitation of Diatomic Molecules

We assume that the lasing molecular species can be described by a diatomic, harmonic oscillator model. The Landau and Teller[7,8] model gives the rate equation as a function of the coefficients for vibrational-translational (V-T) and for vibrational-vibrational (V-V) energy transfer in molecular collisions. These are introduced below[8]:

25

$$\frac{dx_n}{dt} = ZP_{10}^{V-T}\{(n+1)x_{n+1} - [(n+1)e^{-\theta_0} + n]x_n + ne^{-\theta_0}x_{n-1}\}$$

$$+ ZP_{10}^{V-V}\{(n+1)(1+\alpha)x_{n+1} - [(n+1)\alpha + n(1+\alpha)]x_n$$

$$(20)$$

$$+ n\alpha x_{n-1}\} + n_eP_a\{(n+1)x_{n+1} f(u_a - V_a) - [(n+1)$$

$$f(u_a) + n f(u_a - V_a)]x_n + n f(u_a)x_{n-1}\} - R(\delta_{n,\ell+1} - \delta_{n,\ell})$$

Here, x_n is the fractional occupation of the nth vibrational level of the diatomic molecule. ZP_{10}^{V-T} gives the rate of V-T relaxation; θ_0 is related to the gas temperature T_0 by

$$\theta_0 = \frac{\hbar\omega_a}{kT_0} = \frac{V_a}{kT_0}$$

where $\hbar\omega_a$ is the energy separation of the vibrational levels. ZP_{10}^{V-V} gives the rate of V-V relaxation; α is a measure of the energy in vibrational levels.

$$\alpha = \sum_0^\infty nx_n \qquad \sum_0^\infty x_n = 1$$

The term proportional to n_eP_a gives the direct excitation and de-excitation of vibrations by electron impact. The excitation of the vibrational levels is known to proceed via an intermediate ionic state. The cross-section for vibrational excitation by electron impact shows a series of peaks above a certain threshold energy, with increasing energy. The peaks at higher energies correspond to excitation of the higher vibrational levels of the molecule from its ground state.

26

Here we do not consider precisely such a process. We allow only for vibrational excitation by the electrons in single quantum jumps. This assumption lumps the entire excitation cross-section at the sharply defined energy u_a. This assumption is less severe than may appear at first. The only result of the analysis that finally matters is the net excitation rate of the different vibrational levels. The way these rates are produced may be chosen rather arbitrarily, mathematical convenience being one of the criteria for the choice. The mathematically most convenient model is to assume that the cross-section increases with increasing n as done in Eq. (20).

An equation for the energy parameter α may be obtained from (20) by a simple manipulation. We multiply each equation in the set by n and sum. When the summations are evaluated, the V-V transfers disappear because they do not change the total energy in vibrational whatever their distribution. The result is

$$\frac{d\alpha}{dt} + \frac{\alpha - \alpha_o}{\tau_a} - \nu_a^M + R = 0 \qquad (22)$$

where we have defined the relaxation rates

$$\frac{1}{\tau_a} \equiv z P_{10}^{V-T} (1 - e^{-\theta_o}); \quad \nu_a^M = n_e P_a \{ (1 + \alpha) f(u_a) - $$

$$\alpha f(u_a - V_a) \}, \qquad (23)$$

and α_o is defined by

27

$$\frac{\alpha_o}{1+\alpha_o} = e^{-\theta_o}$$

Equation (22) is essentially the energy conservation equation of molecular excitation.

If we had assumed an excitation cross-section for vibrational excitation by the electron that is independent of vibrational level, we would have had to make the additional assumption of a Boltzmann distribution of the vibrational states in order to carry out the summation. Upon evaluation, we would have found

$$\nu_a^{M} = \frac{n_e P_a}{1+\alpha} \ \{(1+\alpha) \ f^{\cdot}(u_a) - \alpha \ f(u_a - V_a)\}$$

Hence P_a of the previous expression is replaced by $\frac{P_a}{1+\alpha}$.

Equation (22) then incorporates everything we need to know about the effect of the electrons and the laser field upon the vibrational system. We have introduced in the above, two vibrational excitation rates, ν_a and ν_a^{M}. The number of electron collisions per unit volume is

$$\nu_a n_e = \nu_a^{M} N_M$$

which must be equal to the number of exciting collisions ν_e^{M} of the molecular species of density N_M

$$\nu_a^{M} = \frac{n_e}{N} \ (\frac{N}{N_M}) \nu_a = \frac{n_e}{N} \ \frac{\nu_a}{C_M} \tag{24}$$

28

where $c_M^| = N_M/N$ is the $\overline{\text{mole}}$ fraction. Now ν_a itself depends upon the operating conditions. This dependence is discussed below.

From (22) it is clear that the rate of energy supply to the lasing gas by the electrons is

$$N_M \nu_a^M V_a = n_e \nu_a V_a = V_a n_e P_a N_M \{(1 + \alpha) f(u_a)$$

$$- \alpha f(u_a - V_a)\} \tag{25}$$

Now, from Eq. (16) we obtain $f(u_a)$ and $f(u_a - V_a)$ for given $\nu_a V_a$. Introducing this into Eq. (25) and solving for ν_a results in

$$\frac{\nu_a}{\nu_x} = \xi_a \frac{V_x/2u_d}{1 + \xi_a \alpha (V_x/2u_d) r_a} \tag{26}$$

where

$$2u_a(1 - \sqrt{\frac{u_a}{u_x}}) = u_a' \simeq \frac{8}{7} u_a \qquad r_a = \frac{V_a}{u_a'}$$

and

$$\xi_a = \frac{3P_a C_M N}{2\nu_c u_a^{3/2}} \frac{u_a'}{V_x} \tag{27}$$

The model with excitation cross-sections independent of vibrational level would have resulted in a similar expression, with ξ_a replaced by $\xi_a/(1+\alpha)$.

Combining the normalization (18) with (26), one finds expressions

$$\nu_x = \frac{\nu_c 2u_d}{V_x} \frac{2u_d + \xi_a r_a V_x}{2u_d + \xi(V_a + \alpha r_a V_x)} \tag{28}$$

$$\nu_a = \nu_c 2u_d \frac{\xi_a}{2u_d + \xi_a(V_a + \alpha r_a V_x)} \tag{29}$$

29

Some interesting features may be noted in expressions (28) and (29). For a very large u_d (or E/N), and $\alpha = 0$, ν_a approaches $\xi_a \nu_c$. Thus ξ_a expresses the rate of vibrational excitation at high fields in terms of the elastic collisions when all molecules are in the ground vibrational state.

Next, we note that ν_a and ν_x approach zero when E/N → 0 (u_d → 0). This is clearly as it must be. From this fact one may obtain a check on (28) and (29). Note that $\nu_x \propto u_d^2$ and $\nu_a \propto u_d$, when $\alpha = 0$ and u_d → 0. Because of the normalization (18), we find

$$\frac{\nu_a}{\nu_c} = \frac{2u_d}{V_a}$$

which checks (29) for $\alpha = 0$ and u_d → 0.

It is further of interest to note that ν_a decreases with increasing α, for fixed driving field fixed u_d. This is easily understood from the fact that superelastic collisions come into play when $\alpha \neq 0$. These collisions impart energy to the electrons at the expense of the vibrational mode thus decreasing the net rate of energy supply by the electrons, $\nu_a V_a$.

ν_x, on the other hand, is enhanced by increasing α, particularly at low values of u_d. When u_d is low, f(u) has a larger discontinuity at $u = u_a$ than when u_d is high. An increase in α decreases the discontinuity and "lets more electron through to the energy u_x, at which electronic excitations occur, hence increasing the rate ν_x.

30

4. Comparison with Nighan's Results

Nighan[1] has presented detailed computations for the electron distribution in CO. We want to study how the analysis presented here meshes with Nighan's results. In order to make approximations equivalent to his, we assume that all molecules are in the ground state, $\alpha = 0$. From (28) and (29), we obtain:

$$\nu_x = \nu_c \frac{\frac{2u_d}{v_x}}{1+\xi_a \frac{v_a}{2u_d}} \tag{30}$$

$$\nu_a = \xi_a \nu_c \frac{1}{1+\xi_a \frac{v_a}{2u_d}}$$

The excitation rate at large E/N (or u_d) is $\xi_a \nu_c$. Nighan's Fig. 12 gives

$$\nu_a\big|_{E\to\infty} \approx 3 \times 10^{-8} \, N_M = \xi_a \nu_c$$

We may use this one result to find all other dependencies. Thus, for example, the fractional power transfers

$$\frac{\nu_a v_a}{\nu_x v_x + \nu_a v_a} \quad \text{and} \quad \frac{\nu_x v_x}{\nu_x v_x + \nu_a v_a} \left(= 1 - \frac{\nu_a v_a}{\nu_x v_x + \nu_a v_a}\right) \tag{31}$$

behave qualitatively like those shown in Fig. 8 of Nighan[1] for pure CO. The two are equal at a value of u_d given by

$$2u_d = \xi_a v_a$$

31

Introducing the definition of u_d one has for the field at which the two curves cross

$$\left(\frac{E}{N}\right)_{cross} = \sqrt{\frac{m}{e} \frac{\nu_c}{N} \frac{\xi_a \nu_c}{N}} \, V_a \tag{32}$$

We use $\nu_c/N = 3.2 \times 10^{-7}$ (the cross section for elastic collisions in CO peaks at $P_c = 120$ at an electron energy 1.7 eV according to reference 9, and hence $\xi_a = 3/32$. The collision frequency is $\nu_c/N = v \, P_c p/N$, where p is the pressure in torr. A peak collision rate of 3.2×10^{-7} results.) Further $V_a = .2$ volts. Thus,

$$\left(\frac{E}{N}\right)_{cross} = 1.06 \times 10^{-15} \text{ volt cm}^2$$

which compares well with Nighan's results. Figure 5 shows the plot of the fractional power transfer to molecular excitation and Nighan's curve for comparison. The agreement is reasonable; the E/N values are off by about 20% and the efficiency does not decrease as fast in the simplified model. This latter effect may be understood on the basis of the fact that the simplified model possesses a "sink" in energy space at $u \sim u_x$ and hence forces the electron distribution to remain at lower energies.

Next consider the plot of ν_{eff}/N_j of Nighan's Fig. 12 and the plot of $\nu_a/C_M N$ obtained from the simplified model.

32

Figure 6 shows such a comparison. Again we find qualitative agreement. The energy range of the electrons is restricted to $2u_a/5 < u < u_x/5$, which accounts for the sharper dropoff of ν_{eff}/N at low energy levels and the termination of the curve at $u_a/5$ as obtained from the simplified model.

5. Electron Distribution and Pumping in a CO_2 Laser Model

In sections 2 and 3 the electron distribution in a diatomic gas laser was obtained and its interaction with the population distribution of the lasing species was determined. In the CO_2 laser, the lower laser level pertains to a different vibrational mode. In order to analyze laser operation all modes of vibration have to be taken into account separately. In this section we extend the analysis in this way.

The model we adopt here for mathematical simplicity is one in which the molecular gas is represented by two temperatures. For this purpose we consider the nitrogen vibrational levels tightly coupled to the asymmetric stretching mode of CO_2 and treat the two vibrational systems as one. In a similar way, we assume that the symmetric stretching mode of CO_2 is tightly coupled to the bending mode and that both of these are describable by a single vibrational temperature. We further assume that the nitrogen vibrational mode and the asymmetric stretching mode of CO_2 are excited via an intermediate ionic state so that excitation occurs when the electrons have

reached a critical energy u_a ($\approx 2eV$); in excitation they are assumed to lose a portion V_a of this energy. The excitation of the combined symmetric stretching mode and bending mode is assumed to occur by low energy electrons of energy u_b which upon excitation lose an energy V_b. When these simplifying assumptions are made, closed form expressions can be derived for all physical quantities of interest.

The distribution function of the electrons, $f(u)$, again obeys Eq. (15). We supplement the G function representing the effect of inelastic collisions by the contribution of the combined bending symmetric stretching mode excitation characterized by an excitation frequency ν_b. The new G function on the right hand side of (15) is shown in Fig. 7. In addition to supplementing $G_x + G_a$ by a rectangular function G_b representing the bending mode collisions, we return the electrons which excite electronic levels at u_x^-, not at $u = 0$.

$$ - \frac{2}{3} \frac{e}{m} (\frac{E}{\nu_c})^2 \nu_c \, u^{3/2} \frac{df}{du} = -(G_x + G_a + G_b) \qquad (33)\,' $$

Here ν_x is the frequency of electronic excitations assumed to occur when the electrons reach energy u_x^+; ν_a is the excitation frequency of the intermediate ionic state of N_2 which then leads to an excitation of the combined nitrogen vibrational levels and asymmetric stretching mode; ν_b is the

34

frequency of excitation of the combined bending and symmetric stretching modes which occurs when the electrons reach energy u_b^+. See Figure 7 for the G-function. Introducing again the definition for drift energy u_d, (17), the closed form solution for the distribution function is

$$f(u) = \frac{\nu_x}{\nu_c} \frac{3}{2u_d} \left(\frac{1}{\sqrt{u}} - \frac{1}{\sqrt{u_x^+}}\right) \equiv f_1(u); \quad u_a < u < u_x^+$$

$$f(u) = f_1(u) + \frac{\nu_a}{\nu_c} \frac{3}{\cdot 2u_d} \frac{\nu_a}{2u_a^{3/2}} \equiv f_2(u); \quad u_x^- < u < u_a$$

$$f(u) = f_2(u_x^-) \equiv f_3(u); \qquad u_b^+ < u < u_x^-$$

$$f(u) = f_3(u) + \frac{\nu_b}{\nu_c} \frac{3}{2u_d} \left(\frac{1}{\sqrt{u}} - \frac{1}{\sqrt{u_b^+}}\right) \equiv f_4(u); \quad u_b^- < u < u_b^+$$

$$f(u) = f_4(u_b^-); \qquad 0 < u < u_b^- \tag{34}$$

If one introduces the normalization condition

$$\int_0^\infty f(u) \sqrt{u}\ du = 1$$

one obtains a relationship among the different excitation frequencies

35

$$\nu_x V_x + \nu_a V_a + \nu_b V_b = \nu_c \, 2u_d \tag{35}$$

where $\quad V_x = u_x^+ - u_x^-$

and $\quad V_b = u_b^+ - u_b^-$

Equation (35) is a form of the energy conservation law. On the left hand side appears the rate of energy transfer by the electrons to electronic excitations and vibrational mode excitations and on the right hand side is the rate of energy supply by the electric field to the electrons. Equation (35) is one equation for the three unknowns, ν_x, ν_a, ν_b for a given electric field E. In order to find more relationships one has to study the molecular excitation in greater detail.

6. The Molecular Excitation of the CO_2-N_2 Model

We assume that the distribution of CO_2 over the asymmetric stretching mode (and the nitrogen vibrational distribution), the symmetric stretching mode, and the bending mode are all described in terms of vibrational temperatures. We introduce convenient energy parameters by

36

$$a \equiv \exp\left(-\frac{eV_a}{kT_a}\right) \qquad b \equiv \exp\left(-\frac{eV_b}{kT_b}\right) \qquad s \equiv \exp\left(-\frac{eV_s}{kT_s}\right) \tag{36}$$

where V_i is the energy spacing of the harmonic oscillator mode i, i = a, b, s.

The energy parameter for the symmetric stretching mode, s, is equal to the square of that of the bending mode, $s = b^2$, because the assumption is made that the spacing of the energy levels of the symmetric stretching mode is twice that of the bending mode and that the temperatures of the two modes are the same. It is helpful to introduce additional energy parameters by the definition

$$\frac{\alpha}{1+\alpha} \equiv a \qquad \frac{\beta}{1+\beta} \equiv b \qquad \frac{\sigma}{1+\sigma} \equiv s \tag{37}$$

The energy U in a particular mode is given directly in terms of the Greek letters, e.g. $U_a = \alpha V_a$ The energy conservation relation for the asymmetric stretching mode can be written particularly conveniently in the form

$$n_e V_a = NC_{MN}\left(\frac{d\alpha}{dt} + \frac{\alpha - \alpha_o}{\tau_a} + \frac{C_M}{C_{MN}} R\right) \tag{38}$$

Here τ_a is a phenomenological relaxation time for the asymmetric stretching mode; R is the rate at which vibrational quanta are lost from the system via radiative transitions; n_e is the electron density; N is the particle density; C_{MN} the mole fraction of

37

nitrogen and CO_2 because α describes the combined energy of the asymmetric stretching mode and the nitrogen vibrational mode. In order to write an energy conservation relation for the symmetric stretching mode and the bending mode it is necessary to take note of the degeneracy of the bending mode. The m-th level of the bending mode has the degeneracy m+1. Under these conditions the energy in the bending mode is $2\beta\hbar\omega_b$. The energy in the symmetric stretching mode is $\sigma\hbar\omega_s = 2\hbar\omega_b$. The energy conservation relation for the combined symmetric stretching mode and bending mode is

$$n_e\nu_b = 2NC_M \{\frac{d}{dt} (\sigma + \beta) + \frac{\sigma - \sigma_o}{\tau_s} + \frac{(\beta - \beta_o)}{\tau_b} - R\} \qquad (39)$$

Here we have introduced the two phenomenological relaxation times τ_s and τ_b for the stretching and bending modes respectively. C_M is the mole fraction of CO_2. The arrival of quanta via radiative transitions is contained in R. Equations (38) and (39), using the fact that σ is related to β by

$$\frac{\sigma}{1+\sigma} = (\frac{\beta}{1+\beta})^2 \qquad (40)$$

provide two relations for the two unknowns α and β in terms of ν_a and ν_b. Now, the excitation rates themselves depend on the molecular excitation. One of these dependencies can be taken directly from (26). Indeed, the nature of the excitations and de-excitations at energies lower than u_a does not affect

38

the solution for the distribution function $f(u)$ in the range $u > u_a$, and hence all relations derived from this part of the distribution function remain valid. We have from Eq. (26)

$$\frac{\nu_a}{\nu_x} = \xi_a \frac{\frac{V_x}{2u_d}}{1+\xi_a \alpha \frac{V}{2u_d} r_a}$$

Now, consider the de-excitation of the (m+1)th level to the m-th level of the bending mode by an electron collision as the result of which the m-th level's population is increased.

Assuming that the collision cross-section is $Q_b^{10}(v)$, one has, for the rate of excitation of the fractional population x_m per degenerate mode, x_m/g_m (g_m is the degeneracy) by entry of particles from the level m+1,

$$(m+1) \frac{x_{m+1}}{g_{m+1}} \int 4\pi^2 n_e \, v Q_b^{10}(v) \, f(v) \, dv$$

The factor (m+1) arises from the fact that we assume interaction of the electron with the molecule via a dipole moment of the molecule. Perturbation analysis shows that the cross-section for the m+1 → m transition is proportional to m+1. The rate is further proportional to the fractional population per degenerate energy level of the (m+1)-th level. The term $v Q_b^{10}(v) n_e$ is the collision frequency for a 1 → 0 transition. This expression is conveniently written in terms

of the distribution function $f(u)$

$$n_e(m+1) \frac{x_{m+1}}{g_{m+1}} \int f(u) R_{10}(u) \, du \qquad (42)$$

where $R_{10}(u)$ is $\sqrt{u}v Q_b^{10}(v)$ as a function of u.

In this format it is easy to take account of the Klein-Rossland relation (detailed balance) which states that the rate of up-transitions from the m-th level to the (m+1)-th level is related to the rate of down transitions in that the $f(u)$ of (42) has to be replaced by $f(u + V_b)$ where V_b is the energy loss in an exciting collision. Taking these relations into account, one has

$$\left(\frac{d}{dt} \frac{x_m}{g_m}\right)_{\text{electrons}} = n_e \left\{ (m+1)\frac{x_{m+1}}{g_{m+1}} \int_0^\infty f(u) R_{10}(u) \, du \right. \qquad (43)$$

$$- \frac{x_m}{g_m} \left[(m+1) \int_0^\infty f(u + V_b) R_{10}(u) \, du + m \int_0^\infty f(u) R_{10}(u) \, du \right]$$

$$+ m \frac{x_{m-1}}{g_{m-1}} \int_0^\infty f(u + V_b) R_{10}(u) \, du \left. \right\}$$

If one assumes that the V-V coupling is so strong that thermal equilibrium is established in the bending mode, then one may set

$$x_m = (m + 1) (1 - b)^2 b^m$$

and one may obtain the rate of energy transfer from the
electrons to the vibrational mode by multiplying both sides
of (43) by g_m and adding over all m. The result may be
identified with the rate of energy supply per molecule, i.e. with
$v_b n_e v_b/N C_M$. One has, after carrying out the summation:

$$\frac{n_e v_b}{N C_M} = n_e \, 2\left(\frac{1+b}{1-b}\right) \, [\int_0^\infty f(u + V_b) \, R_{10}(u) \, du$$

$$- b \int_0^\infty f(u) \, R_{10}(u) \, du] \tag{45}$$

As a simplifying assumption one assumes that $R_{10}(u)$ is a
unit impulse (delta) function at u_b^- (compare Figure 5).

$$R_{10}(u) = R \, \delta(u - u_b^-)$$

Now, we may introduce the expressions for $f(u)$ and obtain
for the integrals

$$\int f(u + V_b) \, R_{10}(u) \, du$$

$$= R \, \frac{3}{2u_d v_x^-} \, [\frac{v_x^-}{v_c} \, (1 - \frac{v_x^-}{v_x^+}) + \frac{v_a}{v_c} \, \frac{V_a}{2u_a} \, \frac{v_x^-}{v_a} \,] \tag{46}$$

Here we have introduced for convenience the normalized velocities
v_b^-, v_x^+, etc. which are equal to the square roots of the respective
energies. The other integral giving the superelastic collision
rate is:

41

$$\int f(u)\, R_{10}(u)\, du = R\, \frac{3}{7u_d v_x^-}\, [\frac{v_x^-}{v_c}\, (1 - \frac{v_x^-}{v_x^+})$$

$$+ \frac{v_a}{v_c}\, \frac{V_a}{2u_a}\, \frac{v_x^-}{v_a} + \frac{v_b}{v_c}\, (\frac{v_x^-}{v_b^-} - \frac{v_x^-}{v_b^+})]$$

(47)

One interesting fact emerges from the above relations. The superelastic collision rate contains the factor $\frac{v_x^-}{v_b^-} - \frac{v_x^-}{v_b^+}$ in the square brackets that can be made much larger than unity if $\frac{v_b^+ - v_b^-}{v_b^+}\, \frac{v_x^-}{v_b^-} \gg 1$. This is the case when the electrons experiencing a vibrational collision are returned at energies much smaller than those experiencing an electronic collision, and if $\frac{v_b^+ - v_b^-}{v_b^+}$ is not much less than unity, i.e. the "rectangle" representing G_b is wider than the distance of its left hand edge from the origin when plotted against $\sqrt{u}$.

Introducing these expressions into (45) one has for v_b

$$v_b = \xi_b(1 - b^2)\, \frac{(v_x + v_a r_{ax}) V_x}{(1-b) 2u_d + (1+b) b^5 b r_{bx} V_x}$$

(48)

where we have defined the parameters

$$\xi_b \equiv \frac{6NC_M}{V_x v_c}\, R\left(\frac{v_x^+ - v_x^-}{v_x^+ v_x^-}\right)$$

$$r_{ax} = \frac{V_a}{2u_a}\, \frac{v_x^+ v_x^-}{v_a (v_x^+ - v_x^-)} \qquad r_{bx} = \frac{v_b^+ - v_b^-}{v_b^+ v_b^-}\, \frac{v_x^+ v_x^-}{v_x^+ - v_x^-}$$

(49)

The meaning of ξ_b may be gleaned from some simple observations. Note that (29) shows that in the limit of large fields $(u_d \to \infty)$ and zero vibrational excitation $(\alpha = 0)$, $v_a = \xi_a v_c$

42

Now, in the limit of large fields, in the absence of vibra-
tional excitation ($\alpha = 0$, $b = 0$), (48) shows that

$$\nu_b|_{u_{d\to\infty}} = \nu_c \xi_b \tag{50}$$

The meaning of ξ_b is therefore analogous to that of ξ_a; it
expresses the ratio ν_b/ν_c at high fields, in the absence of
vibrational excitation. Equations (26), (35), and (48) give
three relations for the three unknowns $\nu_x \nu_a$ and ν_b. For
convenience we repeat them below in modified form

$$V_x\nu_x + V_a\nu_a + V_b\nu_b = 2u_d\nu_c$$

$$-\xi_a\nu_x + [\frac{2u_d}{\nu_x} + \xi_a\alpha r_a]\nu_a = 0 \tag{51}$$

$$-\xi_b\nu_x - \xi_b r_{ax}\nu_a + [\frac{2u_d}{\nu_x}\frac{1}{1+b} + \xi_b\frac{b}{1-b}r_{bx}]\nu_b = 0$$

where

$$r_a \equiv \frac{\nu_x^+}{\nu_a^-}\frac{\nu_a^+ - \nu_a^-}{\nu_x^+ - \nu_a^-} \approx \frac{\nu_a}{u_a'}$$

A certain systematic variation may be observed in equations (51).
The diagonal coefficients contain α and b as "feedback", in-
creasing the multipliers, and hence decreasing the corresponding
rates, as the vibrational populations increase. The effects on
the stretching mode and bending mode are different, because dif-
ferent degeneracies have been assumed for the two. The "feed-
back" is smaller the larger $\frac{2u_d}{\nu_x}$, i.e., the larger the

43

electric field. Solving for ν_x, ν_a, and ν_b one finds

$$\frac{2u_d}{\nu_x}\frac{\nu_c}{\nu_x} = 1 + \xi_a\frac{\nu_a}{2u_{db}} + \xi_b\frac{\nu_b}{2u_{db}}\left[1 + \frac{\xi_a r_{ax}\nu_x}{2u_{da}}\right]$$

$$\frac{2u_d}{\nu_a}\frac{\nu_c}{\nu_a} = 1 + \frac{2u_{da}}{\xi_a\nu_a} + \frac{\xi_b}{\xi_a}\frac{\nu_b}{\nu_a}\frac{u_{da}}{u_{db}} + \xi_b r_{ax}\frac{\nu_b}{\nu_a}\frac{\nu_x}{2u_{db}}$$

$$\frac{2u_d}{\nu_b}\frac{\nu_c}{\nu_b} = 1 + \frac{2u_{db}}{\xi_b\nu_b(2u_{da}+\xi_a r_{ax}\nu_x)}(2u_{da} + \xi_a\nu_a) \qquad (52)$$

where $2u_{da} \equiv 2u_d + \xi_a\alpha r_a\nu_x$

$$\left.\begin{array}{l} \\ \\ \end{array}\right\} \qquad (53)$$

and $2u_{db} \equiv 2u_d(\frac{1}{1+b}) + \xi_b\frac{b}{1-b}r_{bx}\nu_x$

As $2u_d\nu_c$ represents the power absorbed per electron these
ratios are reciprocals of the partition of power between
electronic, asymmetric mode and bending mode excitations.
No other power loss has been included in the theory.

It is worth studying some properties of the rates in
the limits of large and small E-field. Consider first the
limit of large E, $u_d \to \infty$ and similarly $u_{da} \to u_{db} \to \infty$

$$\lim_{E\to\infty}\frac{\nu_c}{\nu_b} \to \frac{1}{\xi_b}\frac{u_{db}}{u_d}$$

When the levels are unpopulated, $u_{db} = u_d$ and we find that

$$\lim_{E\to\infty}\nu_b = \xi_b\nu_c; \quad b = 0 \qquad (54)$$

which checks with Eq.(50). When the occupation of the
levels is nonzero, $u_{db} < u_d$ and hence

44

the rate ν_b is larger than the ν_b for $b = 0$. This is the consequence of the fact that the average cross section increases with increasing vibrational temperature. Even though the superelastic collision rate goes up also large-field limit the inelastic collision contribution dominates. Consider next ν_a in the same limit

$$\lim_{E \to \infty} \left(\frac{\nu_c}{\nu_a} \right) \to \frac{1}{\xi_a} \frac{2u_{da}}{2u_d}$$

When the levels are unpopulated, $u_{da} = u_d$ and

$$\lim_{E \to \infty} \nu_a \to \xi_a \nu_c \tag{55}$$

analogous to (54). When the levels are populated, $u_{da} > u_d$ and the rate ν_a goes down. Since we have assumed that the levels associated with ν_a are nondegenerate, the collision cross section does not increase as rapidly as that of the bending mode, and superelastic collisions are relatively more important. They are responsible for the decrease of ν_a with increasing α.

Finally, the limit for ν_x is simply

$$\lim_{E \to \infty} \nu_x = \frac{2u_d}{\nu_x} \nu_c$$

Next consider the limits of the same rates as $E \to u_d \to 0$. Here, one has to decide on the limiting behavior of u_{da} and u_{db} as $u_d \to 0$. This behavior follows from the recognition, confirmed by the evaluation to follow, that v_a is proportional to u_d^2, whereas v_b is proportional to u_d. Therefore, α, which is proportional to v_a, is proportional to u_d^2 and, therefore, $u_{da} \to u_d$ as $u_d \to 0$. Using this fact, one finds

$$\lim_{E \to 0} v_b = \frac{2u_d}{v_b} v_c$$

$$\lim_{E \to 0} v_a = \frac{4u_{db}u_d}{\xi_b r_{ax} v_b v_x}$$

$$\lim_{E \to 0} v_x = \frac{8u_d \, u_{da} \, u_{db}}{\xi_a \xi_b \, v_b v_x^2 \, r_{ax}}$$

7. The V-I Characteristic for an E-Beam Laser[10, 11, 12]

In this section we shall apply the previously developed formalism to an E-beam laser. Because certain approximations have already been made in obtaining Eqs. (52), the present analysis will apply only to the quasi-CW operation of the laser in which the two temperature description of the vibrational modes is adequate. Clearly, an extension of the analysis presented here could cover the five temperature model with attendant complications. Also, we have damped the gas temperature to room temperature.

The electron density in an E-beam laser is prespecified by the E-beam excitation. This makes the determination of the V-I characteristic particularly easy.

From power conservation one has

$$E J = e n_e (V_x \nu_x + V_a \nu_a + V_b \nu_b) \tag{56}$$

which serves to evaluate J in terms of the rates determined earlier. We introduce the normalization condition (35) and obtain

$$J = \frac{2 u_d \nu_c e n_e}{E} \tag{57}$$

Now, n_e is prespecified, $u_d \propto E^2$. Therefore, the relation between J and E is a linear relation with σ given by

$$\sigma = \frac{e^2 n_e}{m \nu_c}$$

regardless whether lasing occurs or not. This fact is rather important. We conclude that the V-I characteristics of the sustainer voltage electrodes would remain unchanged in the presence or absence of lasing. What happens is, that for a given power input per unit volume all the lasing does is to redistribute the flow of energy among the levels, changes ν_x, ν_a and ν_b, changes the electron distribution, but does not affect the conductivity of the medium.

The normalization condition would contain one additional elastic-collision loss term. The J-E relation, however, would still be linear and have the same form as (54).

We may ask what assumption in the above model led to the result of a σ independent of laser action. In general the conductivity is given by

$$\sigma = -\frac{2}{3} \frac{n_e e^2}{m} \int_{f(o)}^{o} \frac{u^{3/2}}{\nu_c} \, df = \frac{2}{3} \frac{n_e e^2}{m} \int_{0}^{\infty} f \, d \frac{u^{3/2}}{\nu_c}$$

so that the above formula results for a constant ν_c whatever the distribution $f(u)$. Lasing, or any other energy loss, usually decreases the mean energy of the distribution. As $\nu_c(u)$ is generally an increasing function of u, lasing may be expected to increase the conductivity and the plasma may take more power from a constant voltage source.

8. Gain and Efficiency of an E-Beam Laser

The operation of an E-beam laser [10, 12] is modelled
by Eqs. (52) which give the excitation rates ν_b, ν_a and ν_x
in terms of the sustainer field E and the temperatures of
the vibrational modes. The conservation equations for the
molecular systems (38) and (39) give the vibrational temperature fac-
tors a,b in terms of ν_b, ν_a and R -- the rate of lasing
transitions. The gain constant α_g of the P(J)-transition
of the laser is obtained from

$$\alpha_g = \frac{\lambda^2}{4\pi} AT_2 \quad (2J - 1) \frac{2B}{kT_0} \{N_{001} \exp[-BJ(J - 1)/kT_0]$$

$$- N_{100} \exp[-BJ(J + 1)/kT_0]\}$$

where A is weakly J-dependent. Stacz et al. [12] have
computed $A = .23$ sec^{-1}. Until now we did not need to
make any assumption about the distribution of the mole-
cules over the vibrational states. The equations in-
volved energy supplied or taken out of the vibrational
modes and gave full information concerning these energy
rates. In order to evaluate the laser population inver-
sion, it is necessary to make the assumption that the
molecules are distributed over their vibrational states
according to the Boltzmann distributions. Then, N_{001},
the population of the quantum state 001, has the probability

$$(1 - a)(1 - b)^2(1 - s)a$$

The probability of the 100 state is

$$(1 - a)(1 - b)^2(1 - s)s$$

$s = b^2$, and thus,

$$N_{001} = N\, C_M\, (1 - a)(1 - b)^2(1 - b^2)\, a$$

and

$$N_{100} = N\, C_M\, (1 - a)(1 - b)^2(1 - b^2)\, b^2$$

We may thus compute the gain as a function of the electric field and R. We show the result in Fig. 8 for no laser radiation, $R = 0$. The values of the physical parameters used to obtain the gain are displayed in Table I. The efficiency is

$$\eta = \frac{N\, C_M\, \hbar\omega_\ell\, R}{n_e(\nu_b V_b + \nu_a V_a + \nu_x V_x)}$$

The plot of η vs E/N is also shown in Figure 9 for different values of percent ionization ($n_e / N\, C_M$) for the case when R is such as to halve the gain, and also when R is so large as to have reduced the gain to zero.

Figure 10 shows the rates ν_b, ν_a and ν_x as functions of E/N, for varying percent ionizations, for the three values of R: $R = 0$, R such that α_0 is reduced to half its $R = 0$ value, R at $\alpha_0 = 0$. We note from Figures 10 that the ν's are roughly independent of the percent ionization and the rates of excitation per unit volume are proportional to n_e. The rates "droop" at the lower values of E/N with increasing laser excitation, the droop being the less the larger the percent ionization. This may be understood from the fact that the "loading" of the electron distribution by the molecular pumping and lasing is the less severe the higher the percent ionization.

50

9. Extension to Study of Self-Sustained Discharge Characteristics

The present formalism can be extended to study laser action in self-sustained discharges. The rate of ionization ν_i is related to the rate of electronic excitation

$$\nu_i = \kappa \nu_x e^{-Bp/E} \tag{58}$$

where B is now one of the Stoletow constants, and p is the pressure. The ionization frequency itself is determined by diffusion and recombination losses:

$$\nu_i = \alpha_r n_e + D/\Lambda^2 \tag{59}$$

where D is the diffusion constant α_r is the recombination coefficient and Λ is a parameter proportional to the discharge tube radius [12]. The other pertinent equations are Eqs. (52) for ν_b, ν_a and ν_c, and Eqs. (38) and (39) involving α and β.

For a given E/N, laser radiation (R), gas temperature (α_g, β_g), and tube geometry, Eqs. (52), (38) and (39) give the five unknowns α, β, ν_b, ν_a, and ν_x in terms of n_e. Eq. (58) gives ν_i; then n_e can be determined from (59). If the system is diffusion dominated $(\alpha_r n_e \ll D/\Lambda^2)$ then Eq. (59)

serves to determine the tube radius R in terms of the electric field (i.e. in this limit the E field is a unique function of R and D). If we want to determine the current, we need an additional equation for J which is provided by (57).

10. Conclusions

The purpose of this paper was to obtain equations for the pumping of molecular systems by electrons in a discharge, and to do this self-consistently so as to take the reaction of the molecular distribution upon the electron distribution into account.

It was found that the normalization condition, which is the power conservation relation for the electrons driven by the electric field, gave one relation between the molecular excitation rate(s) and the electronic excitation rate. The necessary additional relations for the molecular excitation rates were obtained by a detailed study of the inelastic and superelastic collision processes. In this way relations were obtained for the rates in terms of the vibrational population distributions (molecular temperatures). These in turn must satisfy the energy conservation relations for the molecular pumping and relaxation processes. In this way as many equations as unknowns are obtained for the analysis of a discharge with prespecified ionization, such as in the E-beam laser.

52

The E-beam laser provides a simple application for
the formalism. The results obtained from the present analysis
are eminently reasonable. They predict the behavior of a
CO_2 E-beam laser qualitatively and even semi-quantitatively.
It is hoped that the formalism developed here is simple
enough so that it will lend itself to the analysis of prob-
lems involving spatial boundary conditions, flow, diffusion,
situations for which a simplified pumping analysis is neces-
sary in order to reduce the analytical task to manageable
proportions.

References

1.   W. L. Nighan, _Phys. Rev. A 2_, pp. 1989-2000, November, 1970.

2.   R. E. Center and G. E. Caledonia, _Appl. Opt._, _10_, pp. 1795-1802, August, 1971.

3.   J. W. Rich, _J. Appl. Phys._, _42_, pp. 2719-2730, June 1971.

4.   W. B. Lacina, Northrop Corporate Laboratories, NCL 71-32R.

5.   S. D. Rockwood, J. E. Brau, W. A. Proctor, G. H. Canavan, IEEE, J.Q.E.,   pp. 120-129, January 1973.

6.   T. Holstein, _Phys. Rev._ 20, pp. 367-384, September, 1946.

7.   L. Landau and E. Teller, _Phys. Z. Soviet_, _10_, pp. 34-41, January, 1936.

8.   A. I. Osipov and E. V. Stupochenko, _Soviet Phys._, Usp. _6_, No. 1, July-August 1963 (translation), or _Usp. Fiz. Nauk_, _79_, pp. 81-113, January 1963.

9.   R. B. Brode, _Rev. Mod. Phys._ _5_, p. 257, 1933.

10. C. A. Fenstermacher, "High Energy Short-Pulse CO_2 Amplifier Systems Based Upon E-Beam Controlled Discharge Pumping," Symposium on High Power Molecular Lasers, Quebec, Canada, May 15-17, 1972.

11. J. D. Daugherty, "Electron Beam Sustainer Lasers,"
     Symposium on High Power Molecular Lasers, Quebec,
     Canada, May 15-17, 1972, and IEEE J. Quantum Electron.,
     8, 594, 1972.

12. C. A. Fenstermacher, M. J. Nucter, W. T. Leland,
     K. Boyer, Appl. Phys. Letters 20, 56 (1972).

13. S. Brown, Basic Data in Plasma Physics, MIT Press,
     2nd printing, 1961.

14. B. M. Christopher, A. A. Offenberger, Can. Journ.
     of Physics, Vol. 50, 368 (1972).

15. T. J. Bridges, H. A. Haus, P. W. Hoff, IEEE Journ.
     of Quantum Electronics, pp. 777-782, November 1968.

Table I

$u_x^+ = 10$ eV $\qquad\qquad V_x = 9$ eV $\qquad\qquad u_a = 2$ eV

$V_a = 0.289$ eV $\qquad\quad V_b = .25\ V_a$

$u_b^+ = 0.077$ eV

$\nu_c/N = 0.47 \times 10^{-7}$ sec^{-1} cm^3 [13]

$\xi_a = 0.076$ [1] $\qquad\qquad \xi_b = 0.107$ [1]

$1/\tau_a = 380$ sec^{-1} [14]

$1/\tau_b = 16,000$ sec^{-1} [14]* $\qquad 1/\tau_s = 0$

$B/kT_o = 0.0019$

$1/\pi\ T_2 = 4.74$ MHz/torr [15]

$\hbar\omega_\ell = 0.12$ eV

He:CO_2:$N_2 = 6.6$:1:.43

* The two relaxation rates of the symmetric stretching
  mode and the bending mode, have been replaced by a
  single rate $1/\tau_b$, the value of which is equated to the
  rate of relaxation of the symmetric stretching mode.
  Since $\sigma \simeq \beta^2$, this corresponds to a linearization of
  Eq. (39).

56

Figure Captions

Figure 1   Role of S_{inel} as source of electrons in energy space

Figure 2   The negative divergence of $G_a + G_x$ balances the (positive) divergence of G_E

Figure 3   The currents G_x and G_a

Figure 4   The distribution function for pumping of an idealized diatomic gas

Figure 5   Nighan's plot of efficiency of molecular excitation compared with present results

Figure 6   Comparison of Nighan's ν_{eff} with ν_a of the present analysis

Figure 7   The current   in energy space, G_E for two molecular excitation cross-sections

Figure 8   The small signal gain of E-beam laser with percent ionization as parameter (the gas temperature is assumed to be room temperature)

Figure 9   Efficiency η vs E/N with percent ionization as   parameter

Figure 10 The rates of excitation, ν_b, ν_a, and ν_x
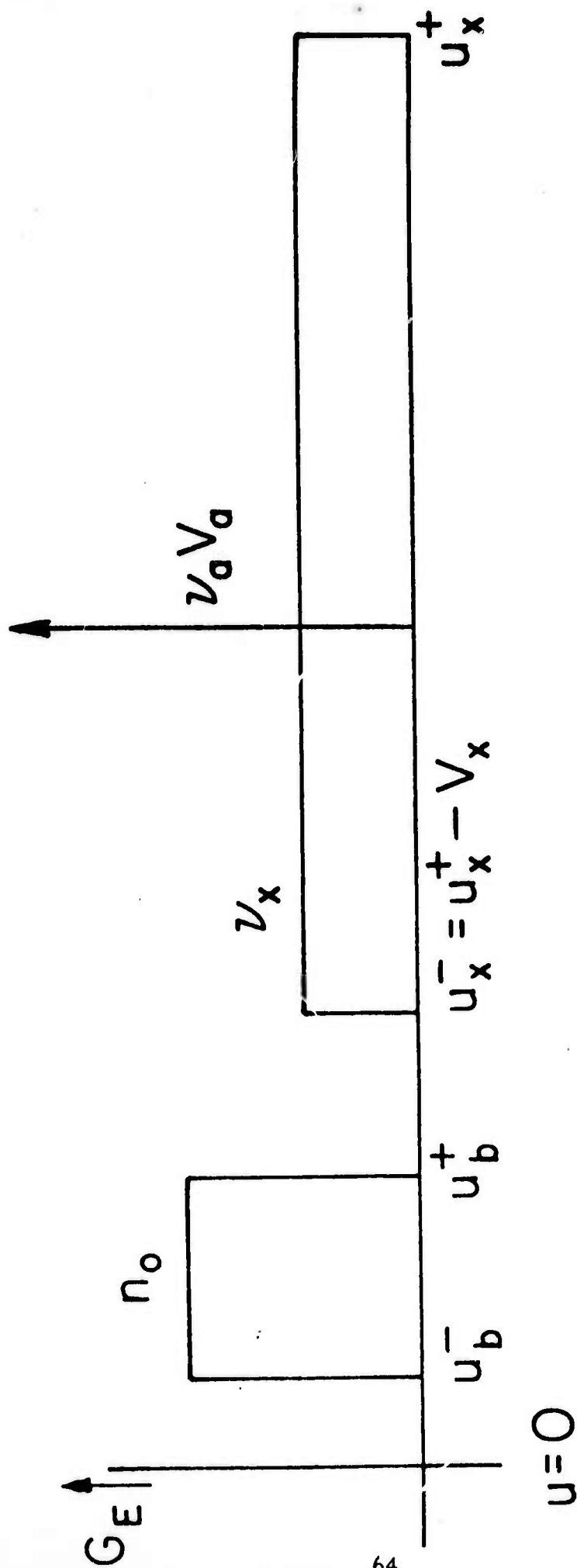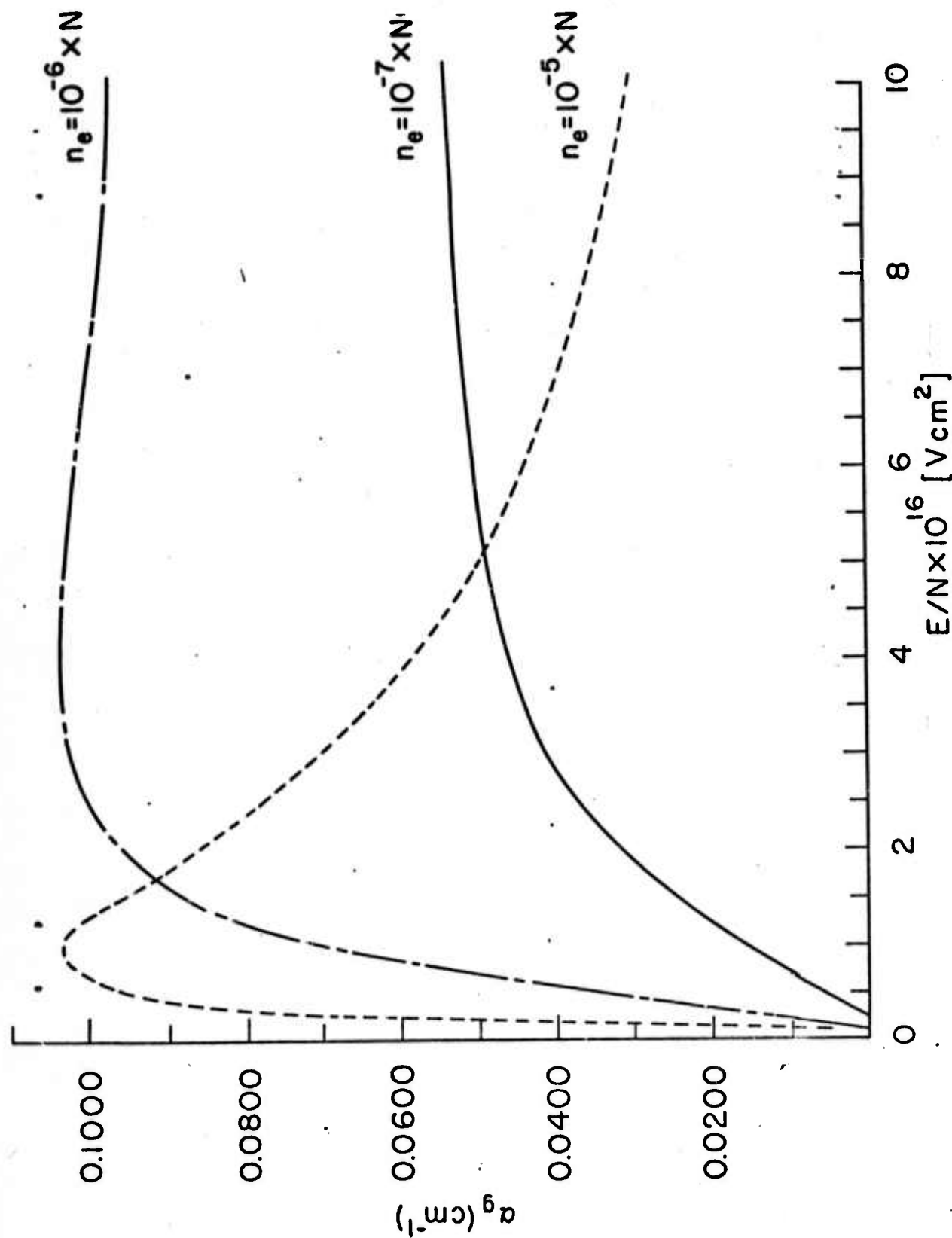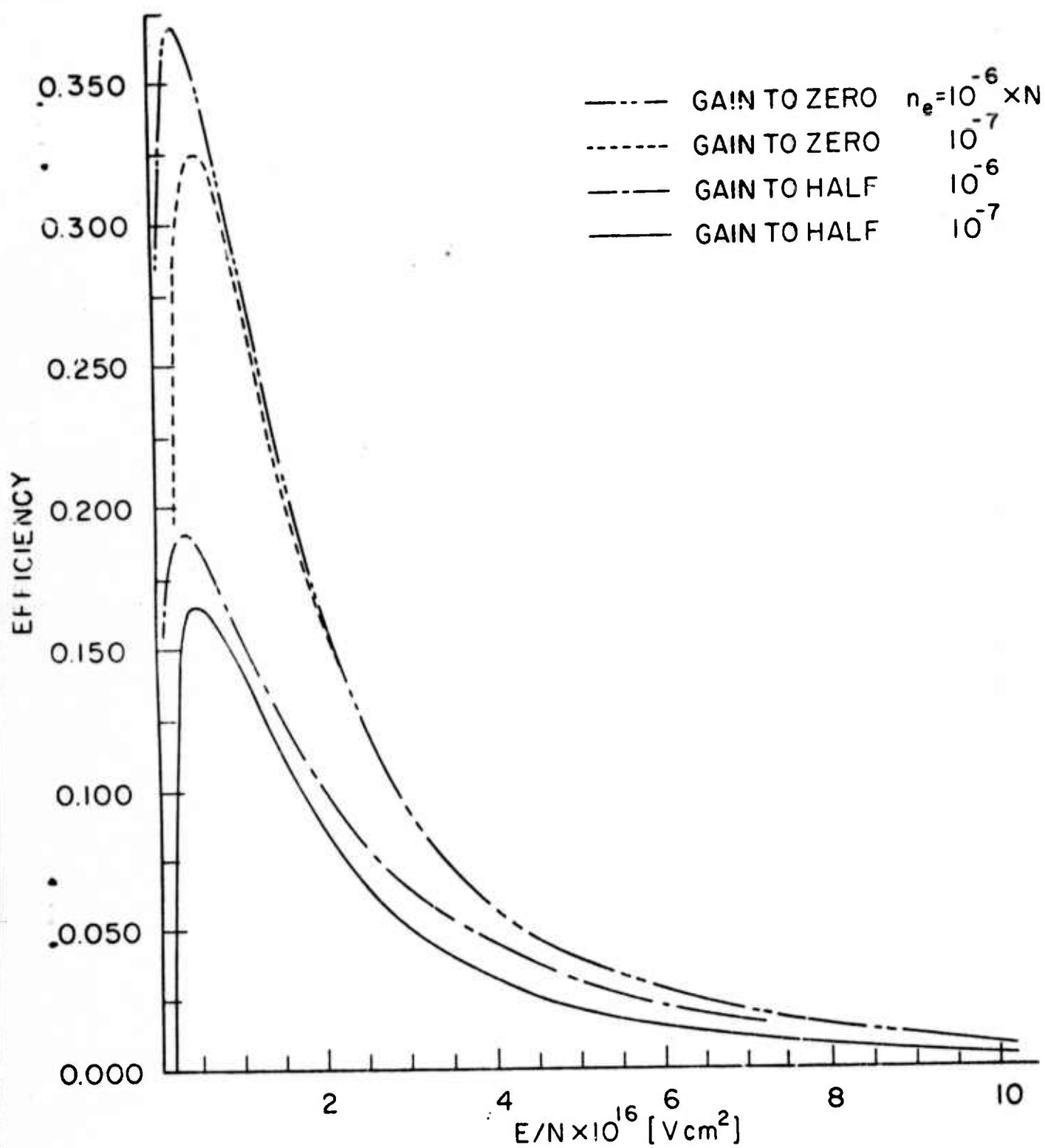
Figure 1

Figure 2

59

Figure 3

Figure 4

Figure 5

Figure 6

63
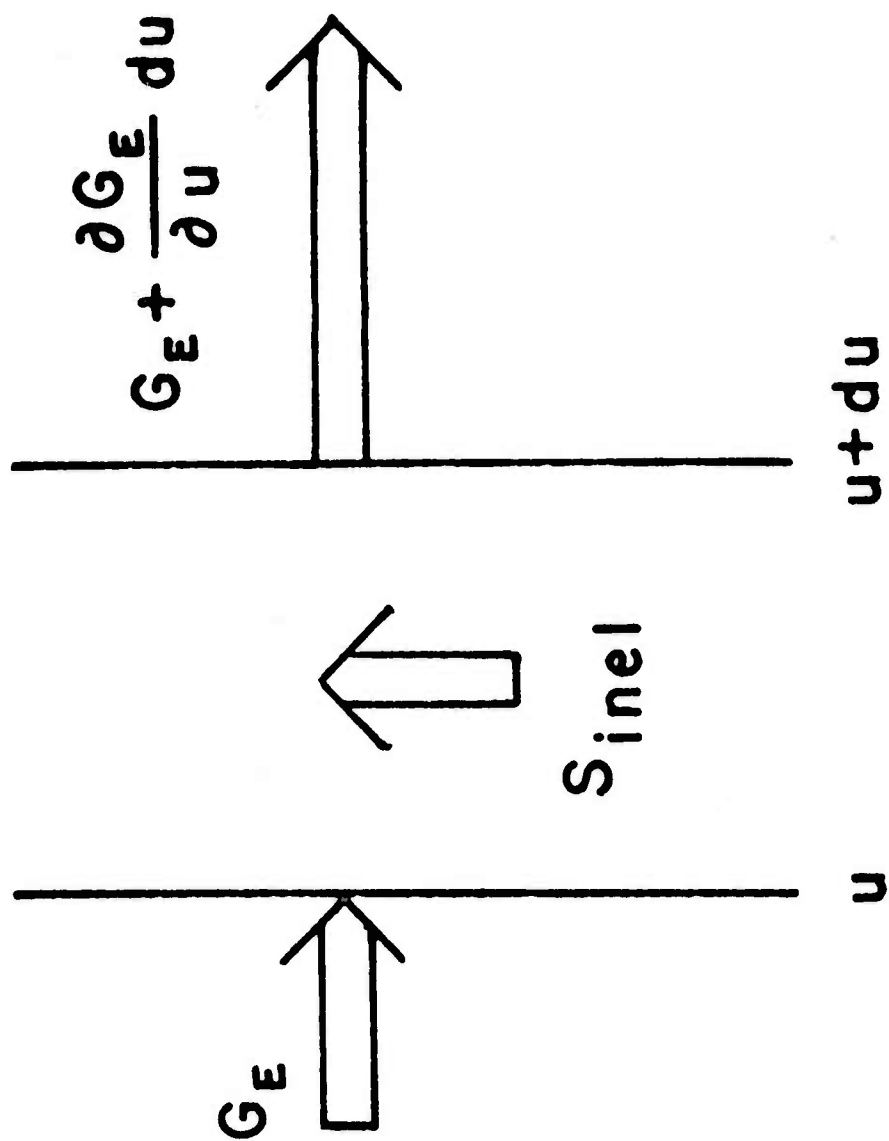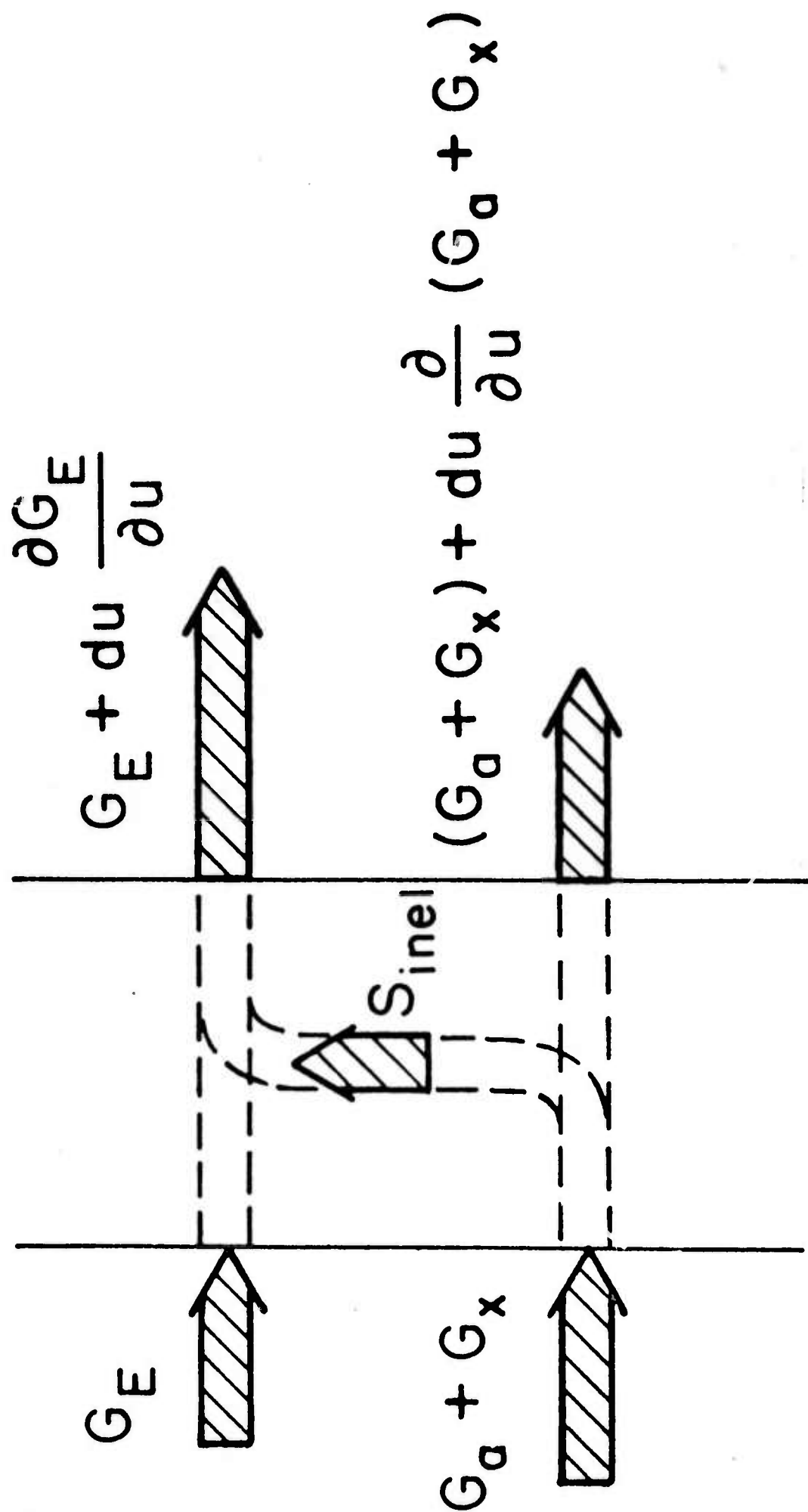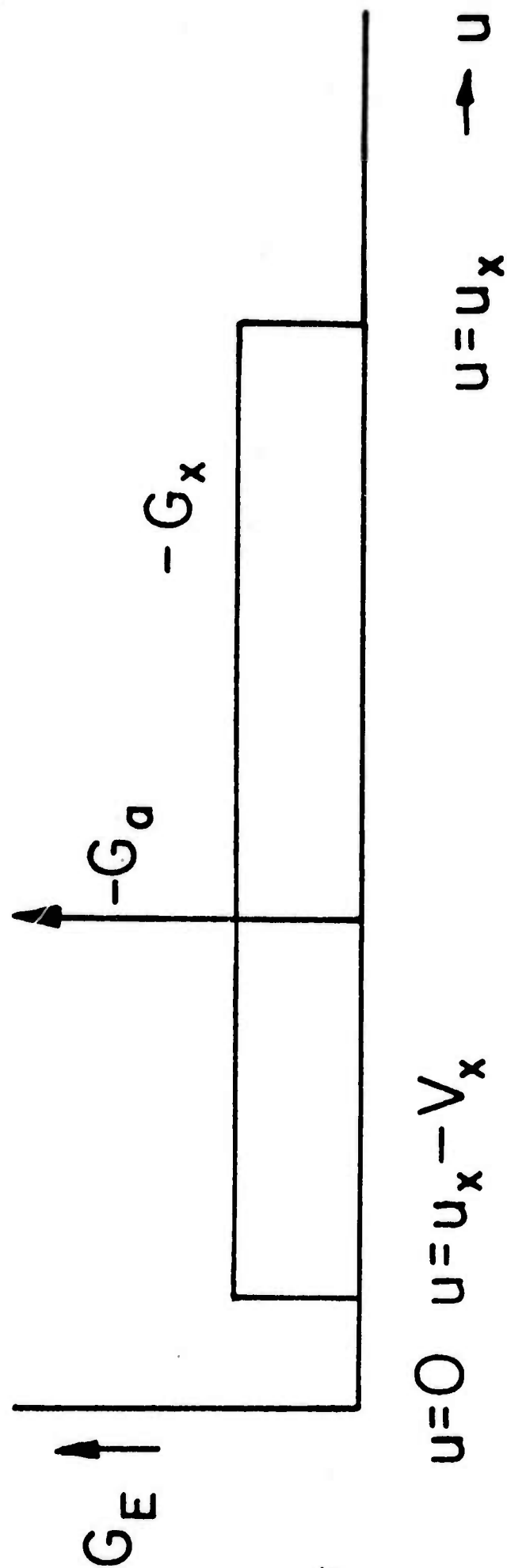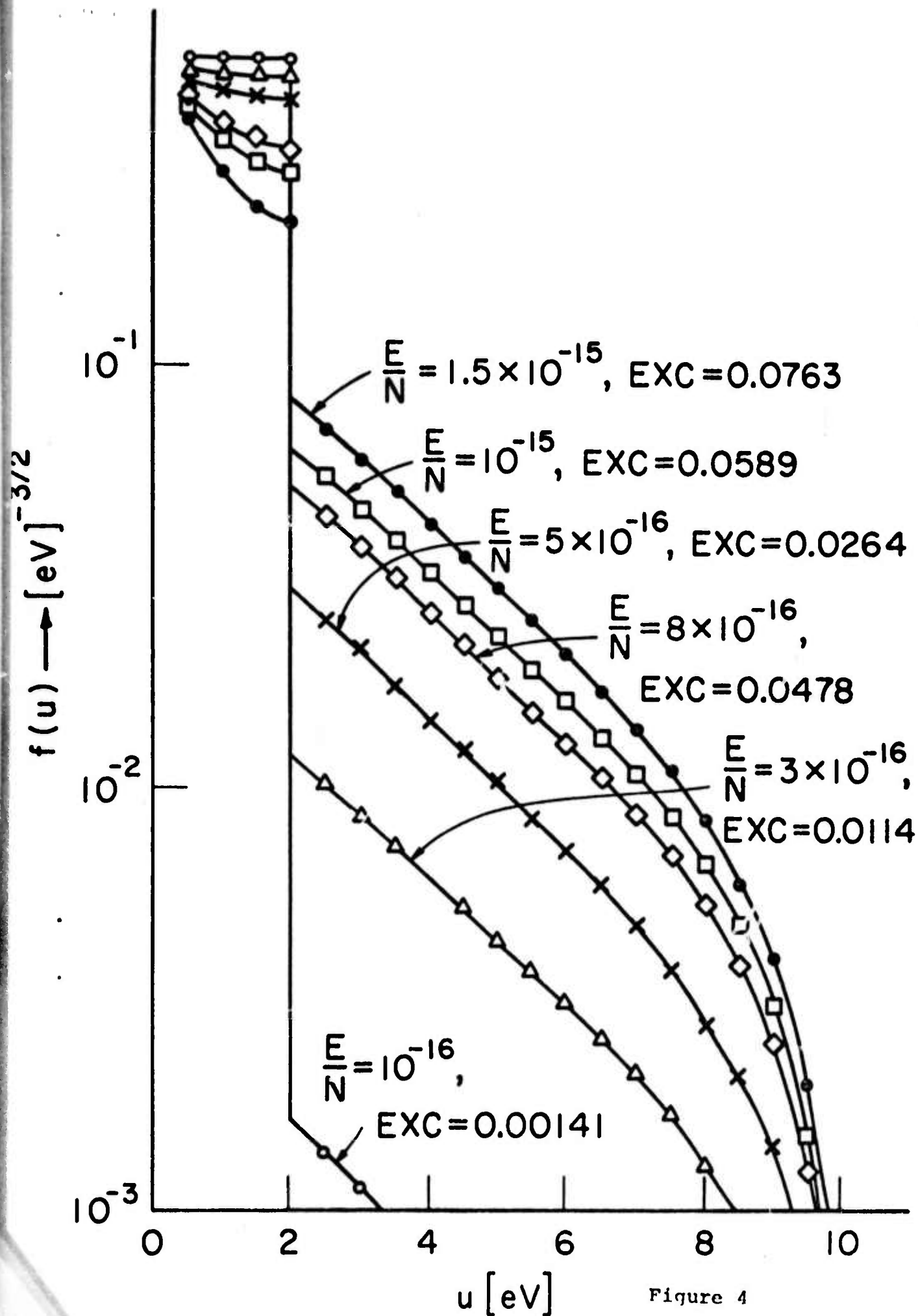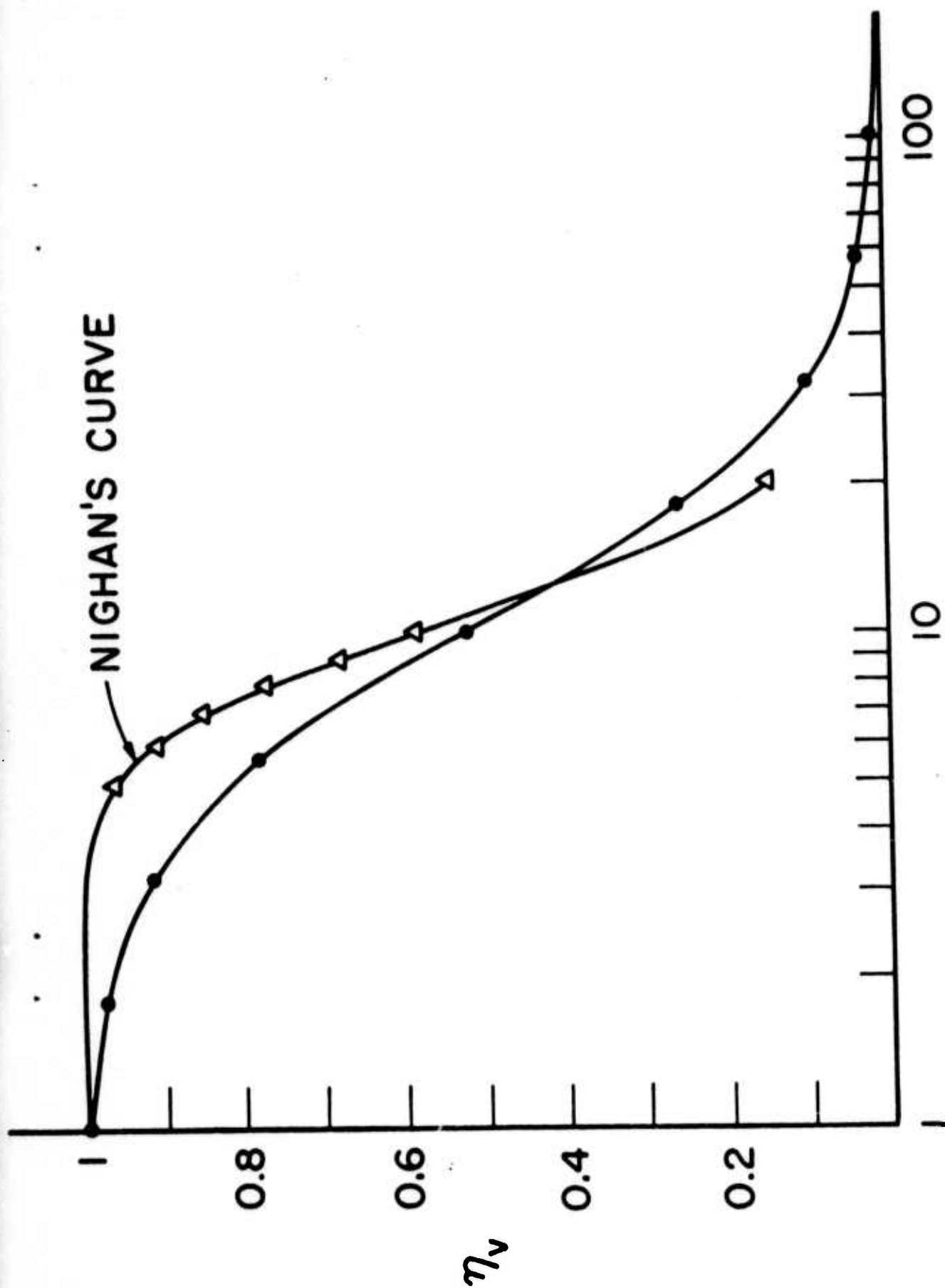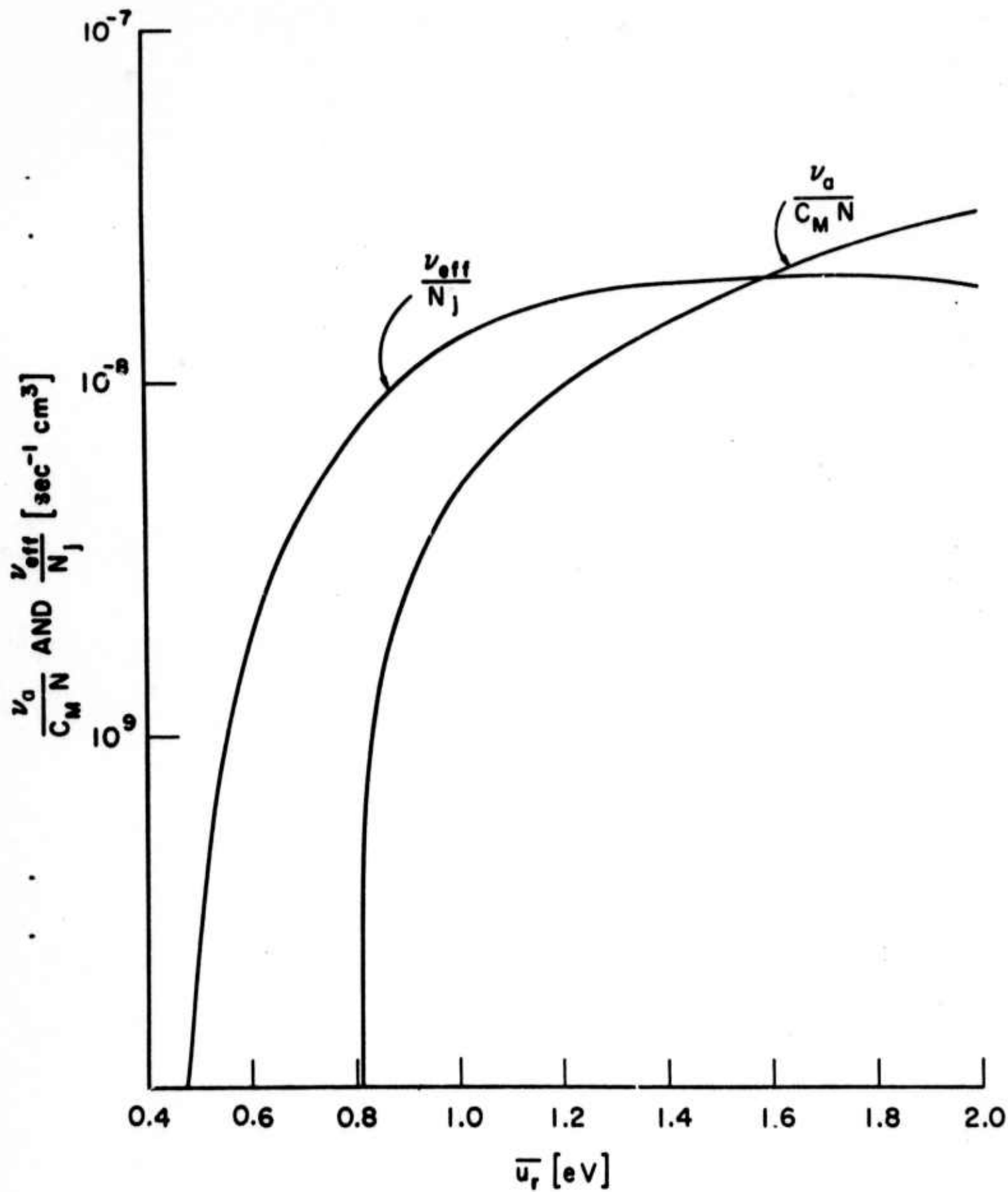
Figure 7

Figure 8

Figure 9

66

Figure 10a

Figure 10b